Inherent rhythm of smooth muscle cells in rat mesenteric arterioles: An eigensystem formulation

I Lin Ho,[1,2,*] Arash Moshkforoush,[3] Kwangseok Hong,[2,4] Gerald A. Meininger,[2,4] Michael A. Hill,[2,4] Nikolaos M. Tsoukias,[3] and Watson Kuo[1,†]

[1]*Department of Physics, National Chung Hsing University, Taichung 402, Taiwan, Republic of China*

[2]*Dalton Cardiovascular Research Center, University of Missouri, Columbia, Missouri 65211, USA*

[3]*Department of Biomedical Engineering, Florida International University, 10555 West Flagler Street, EC 2674, Miami, Florida 33174, USA*

[4]*Department of Medical Pharmacology and Physiology, University of Missouri, Columbia, Missouri 65211, USA*

On the basis of experimental data and mathematical equations in the literature, we remodel the ionic dynamics of smooth muscle cells (SMCs) as an eigensystem formulation, which is valid for investigating finite variations of variables from the equilibrium such as in common experimental operations. This algorithm provides an alternate viewpoint from frequency-domain analysis and enables one to probe functionalities of SMCs' rhythm by means of a resonance-related mechanism. Numerical results show three types of calcium oscillations of SMCs in mesenteric arterioles: spontaneous calcium oscillation, agonist-dependent calcium oscillation, and agonist-dependent calcium spike. For simple single and double SMCs, we demonstrate properties of synchronization among complex signals related to calcium oscillations, and show different correlation relations between calcium and voltage signals for various synchronization and resonance conditions. For practical cell clusters, our analyses indicate that the rhythm of SMCs could (1) benefit enhancements of signal communications among remote cells, (2) respond to a significant calcium peaking against transient stimulations for triggering globally oscillating modes, and (3) characterize the globally oscillating modes via frog-leap (non-molecular-diffusion) calcium waves across inhomogeneous SMCs.

I. INTRODUCTION

Rhythmical contractions in smooth muscle have been observed in many different tissues, e.g., in the gastrointestinal tract, urinary tract, and lymphatic vessels [1–3]. In blood vessels, this activity, named for vasomotion, is found in larger arteries and in low-resistance vessels in microcirculation [4,5], where vascular rhythmicity is apparently synchronous over considerable lengths of arteries [6]. While the literature has investigated the underlying mechanism for many years, it has only been recently that, through images of confocal microscopy, the vasomotion is argued as critically depending on calcium waves originating from intracellular stores [7] and on cell coupling via gap junctions. In addition to these vasomotion phenomena observed in isolated arteries and in some intact mammals (e.g., humans, dogs, rabbits, and rats) [8–11], some operations by *in vitro* experiments indicate that vascular rhythmicity can be enhanced with the help of agonists: noradrenaline (NE), acetylcholine (ACh), phenylephrine (PE), neuropeptide Y, and KCl solution [12–15]. These studies showed that the vasomotion spreads over an increasing distance of the arteriole by raising the dosages of agonists, and tonic contraction can be induced without calcium oscillations at very high concentrations of NE, KCl, and PE; otherwise, the spread of vasomotion is much faster than the movement of molecules by normal diffusion [16], and can be eliminated by clamping the voltage [15].

These physiological reactivities of vascular rhythmicity corresponding to experimental observations are not fully understood. One such inference is that the functionality of vasomotion can be for low-energy-consumption tissue perfusion (1.7 to 8.0 times more efficient than in vessels without vasomotion) [17–19] and could be protective of pathological conditions (e.g., hypertension, via regulating vascular resistance) [20,21]. In this work we investigate vascular rhythmicity by means of mesenteric microcirculation, which is a region of easy-regulating resistance against blood flow. Due to its accessibility, the rat mesenteric artery is one of the most thoroughly studied vascular beds [22,23], bringing forth a vast amount of experimental data. The literature has recognized the need for mathematical models in vasomotion studies and has developed many mathematical models. However, most studies investigated either membrane potential changes or changes in calcium concentrations [24–31], while few works systemically looked at the resonance mechanisms underlying voltage oscillation and the correlated experimental observations with the synchronization of calcium oscillation for smooth muscle cells in rat mesenteric arterioles.

On the basis of experimental data and mathematical equations in the literature, we remodel the ionic dynamics of smooth muscle cells as an eigensystem formulation. By using the first-order Taylor approximation, our approach accurately depicts the characteristic frequencies (eigenvalues) of smooth muscle cells (SMCs) and the correlations of signaling pathways (eigenfunctions) under finite variations of model variables, such as in common experimental conditions. This algorithm provides an alternate viewpoint on frequency-domain analysis and enables one to probe the functionalities of SMCs' rhythm by means of a resonance-related mechanism. However, the

---

*sunta.ho@msa.hinet.net

†wkuo@phys.nchu.edu.tw

first-order approximation could introduce significant numeric inaccuracy if there exist violent fluctuations of variables. Our work mainly investigates the underlying mechanisms of SMCs' rhythmicity by varying dosages of agonists, i.e., potassium, that can diffuse from muscle fibers at the onset of exercise and the responses to evident changes of vascular rhythm [32]. Our calculations show three types of calcium oscillations of SMCs in mesenteric arterioles: spontaneous calcium oscillation, agonist-dependent calcium oscillation, and agonist-dependent calcium spike. For simple single and double SMCs, we demonstrate properties of synchronization among complex signals related to calcium oscillations, and show different correlations between calcium and voltage signals for various synchronization and resonance conditions. For practical cell clusters [30], our analyses indicate that the rhythm of SMCs could (1) benefit enhancements of signal communications among remote cells, (2) respond to a significant calcium peaking against transient stimulations for triggering globally oscillating modes, and (3) characterize the globally oscillating modes via frog-leap (non-molecular-diffusion) calcium waves across inhomogeneous SMCs.

Our conclusions interpret experimental phenomena in the literature and provide materials for understanding other functionalities of calcium dynamics (e.g., appearance of the significant calcium peaking). Our algorithm also offers preliminary considerations for the inherent rhythm of rat mesenteric arterioles at the cell level, which are proposed to have a relation to efficient energy transports and the heart rate [33].

II. MATHEMATICAL ALGORITHMS

A. Basic mathematical modelings

The model is composed of three categories: plasma membrane, cytosol, and intracellular calcium store. Relevant experimental parameters and mathematical equations are derived on the basis of Tsoukias's previous developments for rat mesenteric smooth muscle [22,23]. Figure 1 illustrates a schematic diagram of the model: (i) The dynamics of plasma membrane include ion channels, pumps, exchangers, and receptors, for all the major transmembrane currents that have been identified in SMCs of rat mesenteric arterioles. The ion channels contain a large conductance calcium-activated K^+ channel (BKCa), voltage-dependent K^+ channel (K_v), unspecified leak K^+ channel (K_{leak}), calcium-activated Cl^- channel (Cl_{Ca}), nonselective cation channel (NSC), store-operated cation channel (SOC), voltage-operated Ca^{2+} channel (VOCC), the nonselective gap-junction ion channel (GJ), and the IP_3 gap-junction flux. Specific mathematical descriptions are included for the Na^+-K^+-ATPase pump (NaK), the plasma membrane Ca^{2+}-ATPase pump (PMCA), the Na^+-K^+-Cl^- cotransport (NaKCl), and the Na^+-Ca^{2+} exchanger (NCX). (ii) The intracellular calcium store, representing the sarcoplasmic reticulum, contains sarcoplasmic reticulum Ca^{2+}-ATPase pumps (SERCA), IP_3 receptor Ca^{2+} channel (IP_3R), ryanodine receptor Ca^{2+} channel (RyR), the leak current (leak), and the Ca^{2+} buffering with calsequestrin (CSQN). (iii) The cytosol includes the processes of α_1-adrenoceptor activation and IP_3 formation, incorporated with the effects of NE. The
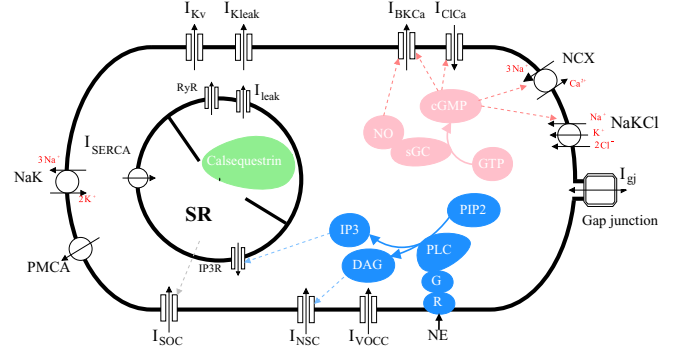

FIG. 1. Schematic diagram of model components for mesenteric smooth muscle cell. BK_{Ca}: Large conductance calcium-activated K^+ channel; K_{leak}: unspecified K^+ leak channel; K_v: voltage-dependent K^+ channel; Cl_{Ca}: calcium-activated Cl^- channel; NSC: nonselective cation channel; SOC: store-operated calcium-permeable nonselective cation channel; VOCC: L-type voltage-operated Ca^{2+} channel; NaK: Na^+-K^+-ATPase; PMCA: plasma membrane Ca^{2+}-ATPase; NaKCl: Na^+-K^+-Cl^- cotransport; NCX: Na^+-Ca^{2+} exchange; SR: sarcoplasmic reticulum; IP_3R: IP_3 receptor; RyR: ryanodine receptor; SERCA: SR Ca^{2+}-ATPase pumps; CSQN: calsequestrin; CM: calmodulin; R: α_1-adrenoceptor; G: G protein; PLC: phospholipase C; sGC: soluble guanylate cyclase; GJ: nonselective gap-junction channel.

vasodilatory action of NO is modeled through a direct effect on the BK_{Ca} channel and through the formation of cGMP. The whole dynamics are integrated by ionic balances for calcium, sodium, potassium, and chloride ions and are described in the Appendix F.

B. Eigensystem formulation for a single SMC

We first consider a single SMC. The 26 transient variables $v_{i \in \{1...26\}}(t)$, having time-dependent evolutions, are re-defined by the function $v_i(t) = \bar{v}_i + \delta_{v_i}(t)$. Here, $\bar{v}_i$ denotes the time average value for variable v_i, and $\delta_{v_i}(t)$ denotes its transient variation. In this work, 26 transient variables for a single SMC are grouped into a vector, i.e., $\vec{v}(t) = ([Ca]_i \ [Ca]_r \ [Ca]_u \ [Na]_i \ [K]_i \ [Cl]_i \ V_m \ d_L \ f_L \ p_f \ p_s \ p_K \ q_1 \ q_2 \ P_{SOC} \ R_{10} \ R_{11} \ R_{01} \ h_{IP3} \ [R_G^S] \ [R_{P,G}^S] \ [G] \ [IP_3] \ [PIP_2] \ V_{cGMP} \ [cGMP])^T$. The 20 relevant ionic currents are also arranged as vector $\vec{I}(t) = (I_{VOCC} \ I_{BKCa} \ I_{Kv} \ I_{Kleak} \ I_{CaNSC} \ I_{NaNSC} \ I_{KNSC} \ I_{SOCCa} \ I_{SOCNa} \ I_{ClCa} \ I_{PMCA} \ I_{NCX} \ I_{NaK} \ I_{NaKCl}^{Na} \ I_{NaKCl}^{K} \ I_{NaKCl}^{Cl} \ I_{SERCA} \ I_{tr} \ I_{rel} \ I_{IP3})^T$ for convenience. Considering finite variations such that the higher-order contributions of variables converge ($\delta_{v_i}^n \to 0$ at $n \gg 1$), ionic currents as well as relevant nonlinear equations can be validly expressed by a Taylor series, e.g., $I_j(t) = \bar{I}_j + \Delta I_j(\bar{v}_i, \delta_{v_i}^n(t))$ for the jth vector component of $\vec{I}(t)$. Here, $\bar{I}_j$ denotes the time average value for component $I_j(t)$.

For the quasiequilibrium conditions, the transient variables $v_i(t)$ and ionic currents $I_j(t)$ are stable and their time-average terms ($\bar{v}_i$ and $\bar{I}_j$) remain constant. All time-dependent behaviors can be attributed to variant terms $\delta_{v_i}(t)$, i.e.,

$$I_j(t) = \bar{I}_j + \Delta I_j(\bar{v}_i, \delta_{vi}(t))$$
$$\simeq \bar{I}_j + \sum_i \Delta I_j^{v_i} \delta_{vi}(t) \qquad (1)$$

for first-order approximation of ionic currents, and

$$\frac{d}{dt}v_i(t) = \frac{d}{dt}\left[\bar{v}_i + \delta_{v_i}(t)\right]$$

$$\simeq \sum_j \Delta^{v_j}_{v_i}\delta_{v_j}(t) + \sum_{j,k}\Delta I_k^{v_j}\delta_{v_j}(t),$$

$$\frac{d}{dt}\delta_{vi}(t) = \sum_{j\in\{1,\ldots,26\}}\left[\Delta^{v_j}_{v_i} + \sum_{k\in\{1,\ldots,20|\}}\Delta I_k^{v_j}\right]\delta_{v_j}(t) \quad (2)$$

for the first-order approximation equations of components $v_{i\in\{1,\ldots,26\}}(t)$, in which relevant variables $\Delta I_k^{v_j}$ and $\Delta^{v_j}_{v_i}$ are derived in more detail in Appendixes B–E. Alternatively, Eqs. (1) and (2) can be formulated in matrix forms:

$$\vec{I}(t) = \vec{\bar{I}} + \mathbf{\Lambda}\vec{\delta}_v(t), \quad (3)$$

$$\frac{d}{dt}\vec{\delta}_v(t) = \mathbf{\Omega}\vec{\delta}_v(t). \quad (4)$$

Obviously, Eq. (4) has an analytical solution:

$$\vec{\delta}_v(t) = e^{\mathbf{\Omega}(t-t_0)}\vec{\delta}_v(t_0), \quad (5)$$

where $\exp(\mathbf{\Omega}t)$ represents the matrix exponential of $\mathbf{\Omega}t$. With the given initial conditions, the transient properties of $\vec{I}(t)$ can otherwise be straightforwardly obtained by substituting Eq. (5) into Eq. (3).

With the eigensolution of the matrix $\mathbf{\Omega}$ in Eq. (4), the transient characteristics of variables $\vec{\delta}_v(t)$ can be conveniently demonstrated from the viewpoint of eigenvalues ω_i and eigenfunction $\vec{\theta}_i(\delta_{v_j})$ for eigenmode i. Without loss of generality, the time evolution of the ith eigenmode can be expressed as $\exp(\omega_i t)\vec{\theta}_i(\delta_{v_j}) \equiv \exp(\omega_{i,r}t + i\omega_{i,c}t)\vec{\theta}_i(\delta_{v_j})$ with $j \in \{1,\ldots,26\}$. The positive (negative) real part $\omega_{i,r}$ of the eigenvalues denotes the growing (decaying) time by $1/\omega_{i,r}$, and the imaginary part $\omega_{i,c}$ denotes its period of oscillation by $2\pi/\omega_{i,c}$. The component amplitude of eigenfunction $|\theta_{i,j}| = |\vec{\theta}_i(\delta_{v_j})|$ indicates the oscillating amplitude of the jth variable v_j in the ith eigenmode, and the phase angle $(\vartheta_{i,j}) = \text{angle}[\vec{\theta}_i(\delta_{v_j})]$ indicates its lag phase in the oscillation period. Since $\mathbf{\Omega}$ is a nonsymmetric matrix, eigenfunctions of SMC systems are not mutually orthogonal in our case.

C. Eigensystem formulation for multiple SMCs

We next consider the condition for multiple (m) SMCs coupled via gap junctions. For this case, Eq. (4) is straightforwardly extended to be

$$\frac{d}{dt}\begin{bmatrix}\vec{\delta}_{v,1}(t)\\ \cdots \\ \vec{\delta}_{v,m}(t)\end{bmatrix} = \begin{bmatrix}\widetilde{\mathbf{\Omega}}_1 & \mathbf{\Theta}_{1j} & 0 \\ \mathbf{\Theta}_{j1} & \widetilde{\mathbf{\Omega}}_j & \cdots \\ 0 & \cdots & \widetilde{\mathbf{\Omega}}_m\end{bmatrix}\begin{bmatrix}\vec{\delta}_{v,1}(t)\\ \cdots \\ \vec{\delta}_{v,m}(t)\end{bmatrix} \quad (6)$$

with matrix components

$$\widetilde{\mathbf{\Omega}}_{pq,i} = \mathbf{\Omega}_{pq,i} + \sum_j \Delta I_{\mathrm{GJ},j}^{v_q}\delta_{v_q,i}, \quad (7)$$

$$\mathbf{\Theta}_{pq,iC} = \sum_j \Delta I_{\mathrm{GJ},j}^{v_q,C}\delta_{v_q,C}. \quad (8)$$

Here, $\Delta I_{\mathrm{GJ},j}$ corresponds to gap junction currents for ion j (or [IP$_3$]) that are in connection with $\delta_{v_p,i}$, and C indexes the nearby SMC coupled to the local one. The component $\widetilde{\mathbf{\Omega}}_{pq,i}$ in Eq. (7) includes additional contributions of the gap junction currents by the terms $\Delta I_{\mathrm{GJ},j}^{v_q}$, which are associated with variations of $\delta_{v_q,i}$ (qth component of $\vec{\delta}_{v,i}$) in the local SMC i. The component $\mathbf{\Theta}_{pq,iC}$ in Eq. (8) includes the contributions of the gap junction currents by the terms $\Delta I_{\mathrm{GJ},j}^{v_q,C}$, that is associated with variations of $\delta_{v_q,c}$ in the nearby SMC C. Since the format of the matrix in Eq. (6) remains the same as that in Eq. (4), the same process for solving a single SMC is applied for multiple SMCs.

III. NUMERICAL RESULTS AND DISCUSSION

In this section, (i) we first carry out the frequency-domain analysis on a control condition of SMCs. We study how the eigenvalue and eigenfunction correspond to time evolutions of transient variables. (ii) Continuing with the frequency-domain approach, we investigate properties of calcium oscillations at different concentrations of potassium; otherwise, we perform the corresponding time-domain analysis to get intuitional ideas of synchronization among complex signals. Another exemplar of two coupled SMCs is prepared to elucidate more realistic (intracellular and intercellular) calcium dynamics and resonance effects. (iii) Lastly, we explore practical finite SMC clusters. With an input delta-function calcium pulse in this resonance medium, we observe physiological functionalities of rhythmic oscillations of SMCs.

Mathematical algorithms were implemented in Visual C++ and were executed on a HP Z800 workstation with 48 GB of RAM. Relevant default values of the variables and initial parameters are defined in Appendix A. Source codes of the C++ language for time-domain and frequency-domain analyses are available online [34]. We also refer to JSim computations for time-domain programming [35].

A. Frequency-domain analysis on the control set of SMCs

Default parameters for the control condition of SMCs are defined in Appendix A, except $[K]_e = 35.8$ mM, $[NE] = 2.0 \times 10^{-4}$ mM, $I_{\mathrm{SERCA},0} = 20.4$ pA, and $R_{\mathrm{leak}} = 0.0000535$. We obtain the equilibrium parameters $\vec{\bar{\delta}}_v$ necessary for frequency-domain analysis after running the time-domain simulation for 10^5 s. Relevant parameters of the SMC model are taken from known experimental measurements [36]: 25 s period calcium oscillation in rat mesenteric arterioles and the threshold value of $[K^+]_e = 20$ nM for triggering calcium oscillation for instance.

Figure 2 shows numerical results of eigenvalues and eigenfunctions for a single SMC on the control condition. The figure is divided into four parts: (a) real parts of eigenvalues that decide the growing time or decaying time of eigenmodes, corresponding to positive or negative values, respectively; (b) imaginary parts of eigenvalues that indicate the oscillation periods of eigenmodes; (c) oscillating amplitude of transient variables in eigenmodes M22 and M23; and (d) oscillating phase of transient variables in eigenmodes that tells the phase lags regarding oscillations. Each oscillating amplitude value in
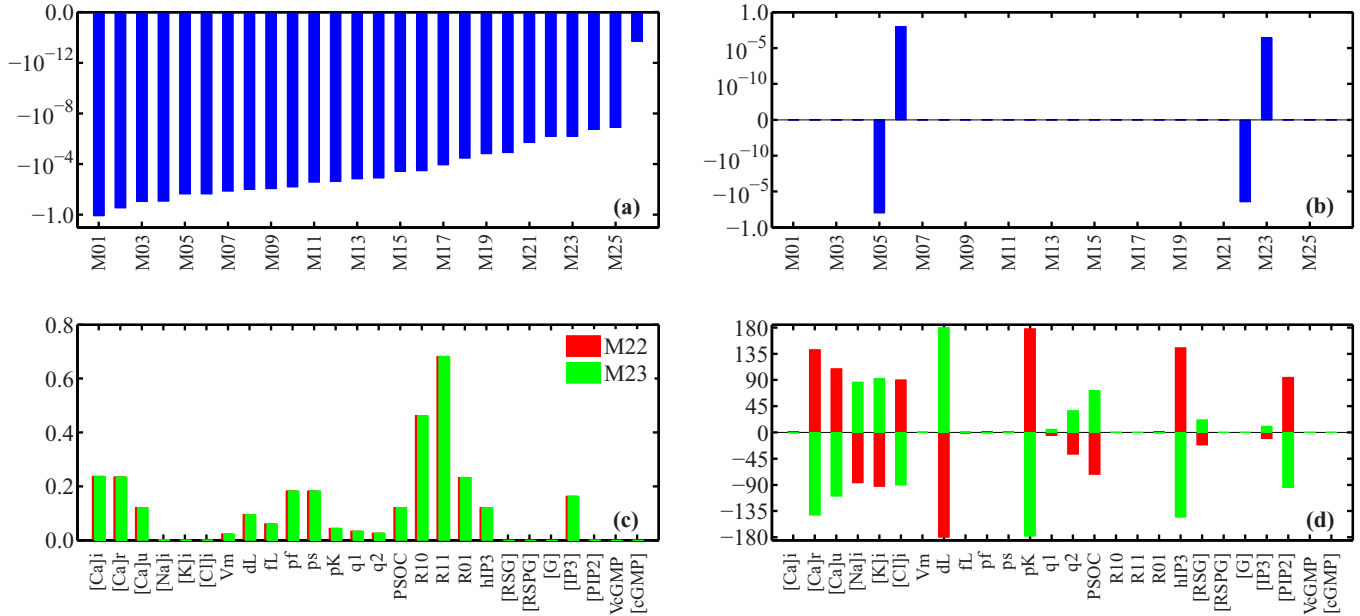
FIG. 2. Numerical analysis of eigenvalues and eigenfunctions for a single SMC on the control condition: (a) real parts of eigenvalues, (b) imaginary parts of eigenvalues, (c) oscillating amplitude of transient variables in eigenmodes 22 and 23, and (d) oscillating phase of transient variables in eigenmodes 22 and 23.

Fig. 2(c) is divided by its own average to show the percentage of variations and is dimensionless.

In Figs. 2(a) and 2(b) for a single SMC model, we obtain two sets of mutually complex-conjugate eigenvalues, with values $-0.028 \pm 0.011i$ and $-8 \times 10^{-7} \pm 0.000264i$ ms^{-1}, corresponding to eigenmodes (5,6) and (22,23), respectively. We select the set of eigenmodes (22,23), which signify a longer decay time of 1250 s and an oscillation period of 23.8 s, for studying the properties of transient variables.

For the set of eigenmodes (22,23), Figs. 2(c) and 2(d) illustrate the oscillating amplitude and phase of transient variables. Several quantities are discussed here for the following study: the oscillation amplitude of [Ca]$_i$ is 22%, the oscillation amplitude of [Ca]$_u$ is 10%, and the phase difference between [Ca]$_i$ and [Ca]$_u$ is 105°.

To apply the quantities from frequency-domain analysis, we study the time-domain calculations. Figure 3 shows numerical results for the time evolutions of several transient variables. Figure 3(a) presents the temporal variation of [Ca^{2+}]$_i$ to arrive at the equilibrium after $t = 4 \times 10^4$ s. After equilibrium, we add an input of delta-function calcium stimulation at $t = 4.8 \times 10^4$ s. Responses to this stimulation illustrate a calcium oscillation having decaying time $1/\omega_{22,r} = -1250$ s [green curve in Fig. 2(a)] and oscillation period $2\pi/\omega_{22,c} = 24$ s [blue curve in Fig. 2(b)], which agree with the values from frequency-domain analysis. An extra calculation for SMCs in experimental conditions ([K$^+$]$_e$ = 40 mM; red curve) is appended here to explain the high dosages of agonists and is in the paragraph below.

Figures 3(c) and 3(d) characterize oscillating amplitudes and phases for several transient variables in eigenmodes (22,23). Here, each curve is divided by its average of variables in order to compare the results with Figs. 2(c) and 2(d): 22% oscillation amplitude of [Ca]$_i$ relatively compared to

10% oscillation amplitude of [Ca]$_u$, and 105° phase lags between [Ca]$_i$ and [Ca]$_u$, which agree with those in Figs. 2(c) and 2(d).

B. Time-domain and frequency-domain analyses for a single SMC

Continuing with the frequency-domain approach, we investigate properties of calcium oscillations at different concentrations of potassium. Figure 4 gives the eigenvalue spectrum of a single SMC in response to different extracellular potassium concentrations. The spectrum is depicted in units of time, instead of frequency, for convenient descriptions. For real parts of eigenvalues in Fig. 4(a), the positive (negative) value denotes the growing (decaying) time $\sim(1/\omega_{i,r})$. We find two sets of complex-conjugate solutions corresponding to rhythmic oscillations by frequency-domain analysis: (i) the set of eigenmode (5,6) (green curves) characterizes a short oscillation period ($\sim$0.1–1 s), fast decay time ($\sim$0.1 s), and insensitivity against agonist. This mode exists even under very low dosages of agonists. According to the literature [6], rat mesenteric arteries are resistant to spontaneous vasomotion. Moreover, only sparse observations of spontaneous vasomotions with periods $\sim$2 s are noted in our experiments of mesenteric arterioles. For these reasons, we identify eigenmodes (5,6) as spontaneous vasomotions and observe them infrequently in realistic mesenteric arterioles due to their fast decay. (ii) The set of eigenmode (22,23) (red and blue curves in Fig. 4), however, exhibits strong dependence on the extracellular potassium concentrations and has different behaviors in regions I, II, and III. In region I, an oscillation-deactivation section, eigenvalues of modes 22 and 23 are real and distinctly separate, and no oscillating actions appear. In region II, an oscillation-activation section, the decay time of modes
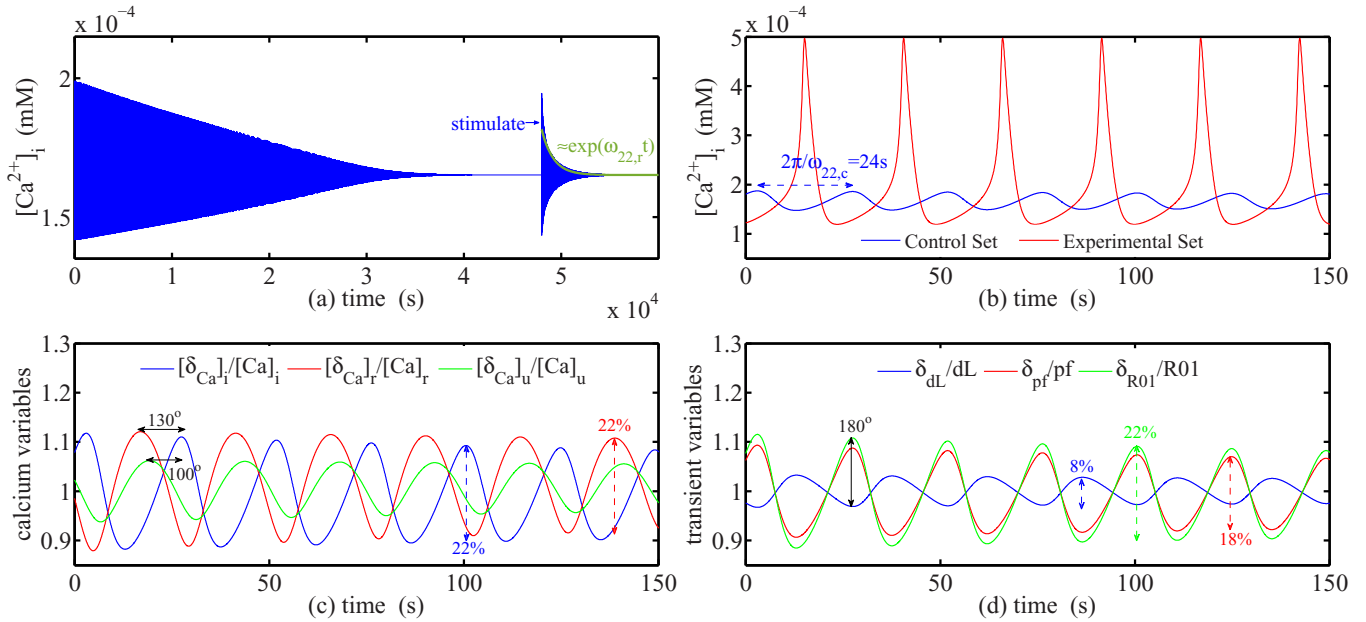
FIG. 3. Time evolutions of several transient variables in eigenmodes (22,23) for a single SMC: (a) time evolution of $[Ca^{2+}]_i$ with given delta-function calcium stimulation at equilibrium $t = 4.8 \times 10^4$ s, (b) transient variations of $[Ca^{2+}]_i$ after the delta-function calcium stimulation for the control condition $[K^+]_e = 35.8$ mM and experimental condition $[K^+]_e = 40.0$ mM, and (c) and (d) transient variations of several variables after the delta-function calcium stimulation.

(22,23) prolongs exponentially when increasing extracellular potassium concentrations, and is present as a dominant eigenmode at $[K]_e \simeq 36$ mM. Around $[K]_e \simeq 36$ mM, the set of eigenmode (22,23) can be realized as experimental observations due to the robustness of its lifetime. For $[K]_e \ll 36$ mM, eigenmode (22,23) could be smeared due to the nature of nonorthogonality to other nonoscillating eigenmodes (gray curves). In region III, as shown in Fig. 4(a), the real part of the eigenvalues turns into a positive value, and hence eigenmode (22,23) transfers to a transient growing type. The oscillating amplitude could rise violently along the temporal curve as the red curve (experimental set) in Fig. 3(b). In this region, the significant deviations from equilibrium values of transient

variables invalidate the precision of our algorithm except for qualitative inferences. In summary, numerical results of Fig. 4 show three types of calcium oscillations for a single SMC in mesenteric arterioles: spontaneous calcium oscillation (green curves), agonist-dependent calcium oscillation (blue curves in region II), and agonist-dependent calcium spike (blue curves in region III) as shown in Fig. 4.

In addition to eigenvalue analysis in Fig. 4, eigenfunctions also provide explicit information as discussed below. Figures 5 and 6 show the oscillating amplitude $\hat{\delta}_{vi} \equiv |\delta_{vi}/\bar{\delta}_{vi}|$ and oscillating phase ϑ_{vi} for eigenmode (22,23) in response to extracellular potassium concentrations, respectively. By Eq. (3), we transform the eigenfunction associated with $\bar{\delta}_v$
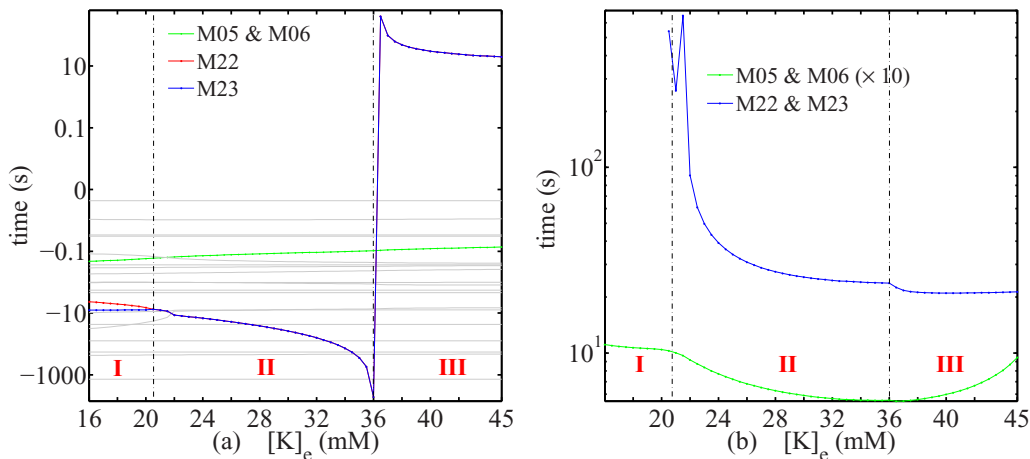

FIG. 4. Eigenvalue spectrum of a single SMC in response to extracellular potassium concentrations. (a) Real parts of eigenvalues for evolution time $\sim 1/\omega_{i,r}$, and (b) imaginary parts of eigenvalues for oscillation periods $\sim 2\pi/\omega_{i,c}$.
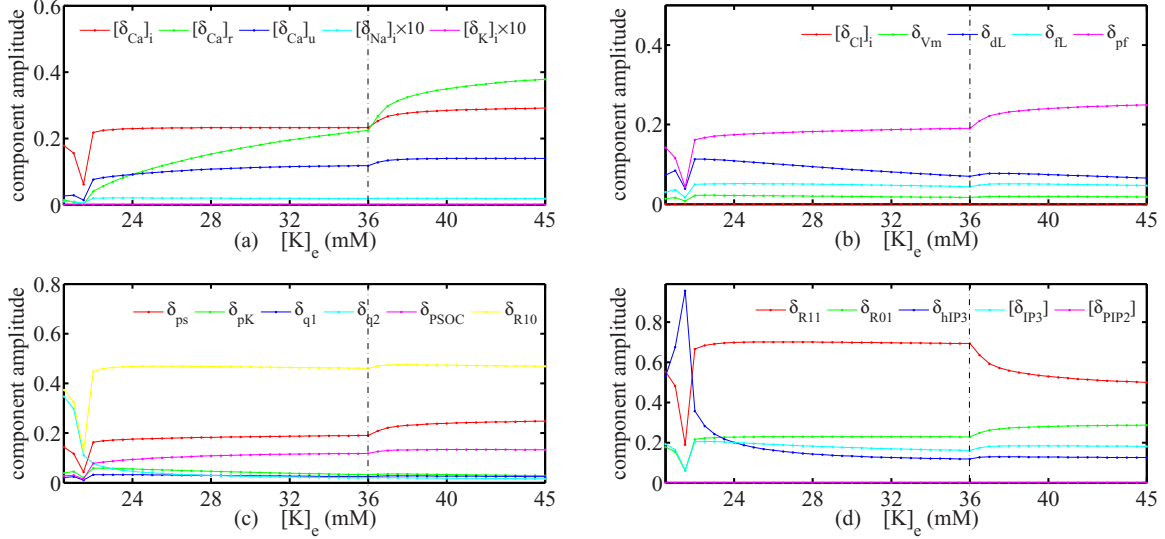
FIG. 5. Oscillating amplitude $\hat{\delta}_{vi} \equiv |\delta_{vi}/\bar{\delta}_{vi}|$ of variables in eigenmode (22,23) in response to extracellular potassium concentrations.

into an eigenfunction associated with currents $\Delta \vec{I} \sim \mathbf{\Lambda} \vec{\delta}_v$. Figures 7 and 8 illustrate numerical results for the oscillating amplitude and phase of currents in eigenmode (22,23) versus extracellular potassium concentrations, respectively. We note that the definitions of phase lag here refer to the calcium oscillation in cytosol.

Previous studies of signal inhibitions and vascular mechanics have in fact suggested a diverse mechanism (in addition to the known intracellular stores) for rhythmic contractions of SMCs. For instance several mechanical measurements [37–42] have demonstrated mandatory or modulatory roles of K^+ channels for vasomotion in arteries. The activation of cGMP and the calcium-dependent chloride current for vasomotion have been found in endothelium-denuded mesenteric arteries. In a voltage-dependent coupled oscillator model, the literature has also proposed the depolarization and the involve-

ment of voltage-dependent calcium current to be responsible for agonist-dependent vasomotion in mesenteric arteries [43–45].

To investigate the interplays of a diverse mechanism for rhythmic contractions of SMCs, we study the correlations and synchronizing timings of signal pathways from Figs. 5–8. We find the following: (i) By increasing $[K]_e$, electrical oscillations in cytosol gradually change from the cyclic $(K_i^+ + Na_i^+ \leftrightarrow Ca_i^{2+} + Cl_i^-)$ configuration toward the cyclic $(K_i^+ + Na_i^+ + Ca_i^{2+} \leftrightarrow Cl_i^-)$ configuration as in Fig. 6. This is in response to the growing strength of oscillations by alternate positive and negative charge accumulations in cytosol at high $[K]_e$. (ii) By increasing $[K]_e$, the oscillating amplitude related to transmembrane currents decreases, while the oscillating amplitude related to intracellular stores $(\Delta I_{tr}, \Delta I_{rel}, \Delta I_{SERCA})$ increase as in Fig. 7. (iii) By increasing $[K]_e$, the oscillating
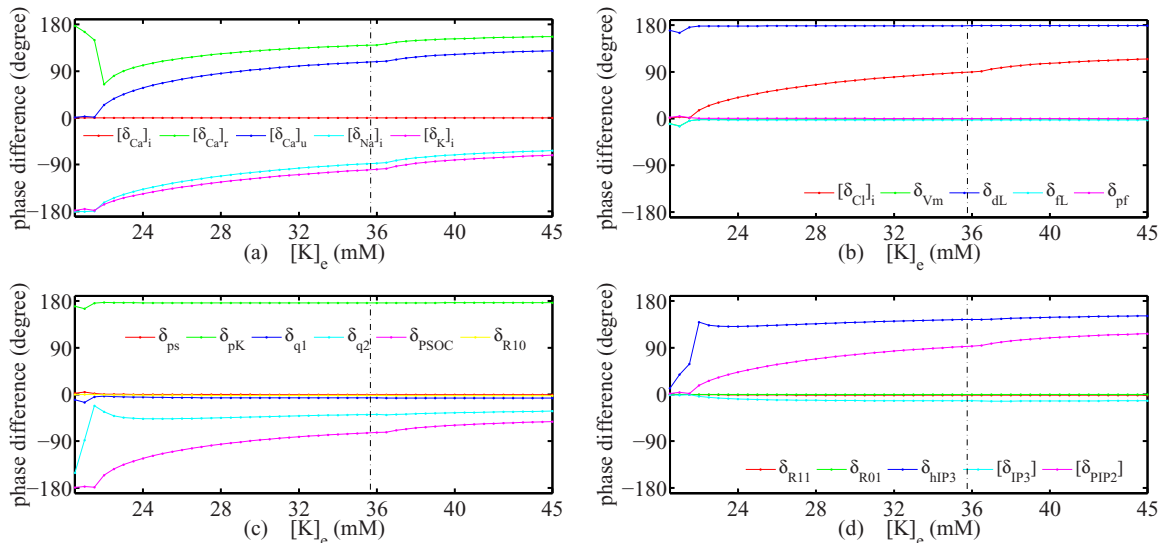

FIG. 6. Oscillating phase ϑ_{vi} of variables in eigenmode (22,23) in response to extracellular potassium concentrations.
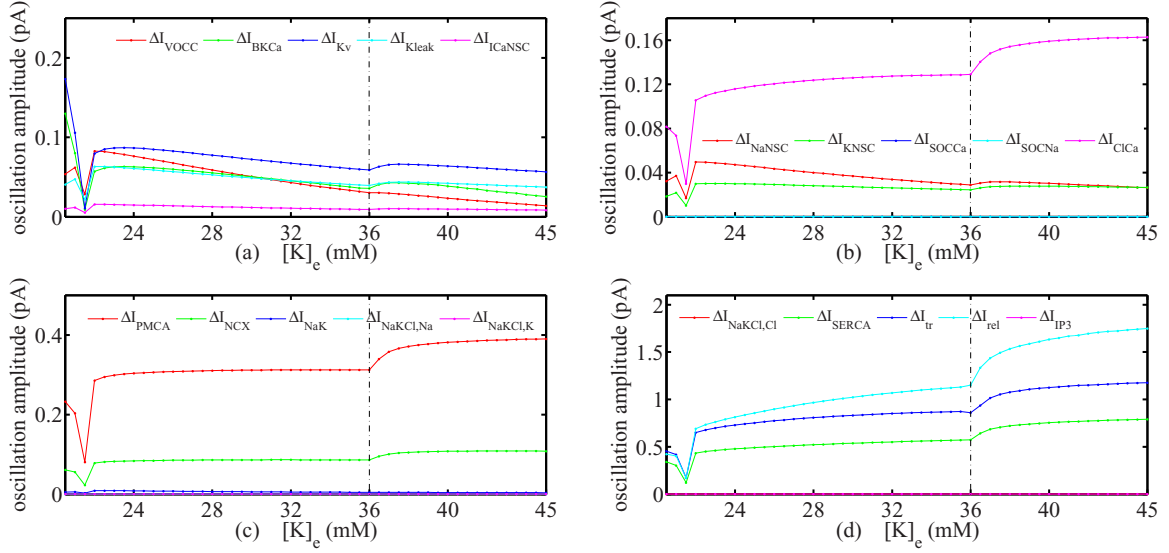
FIG. 7. Oscillating amplitude of current ΔI_i in eigenmode (22,23) in response to extracellular potassium concentrations, in which $[\delta_{Ca}]_i = 2 \times 10^{-5}$ mM.

amplitude of $[\delta_{Ca}]_r$ rapidly increases while that of $[\delta_{Ca}]_i$ and $[\delta_{Ca}]_u$ almost remains constant as in Fig. 5. This fact causes the evolvement of the temporal wave form of $[Ca]_i$ from being a sinelike [e.g., blue curve in Fig. 3(b)] to a spikelike [e.g., red curve in Fig. 3(b)] function, while keeping the accumulation of $[Ca]_i$ (integral area of wave form) relatively stable. (iv) By increasing $[K]_e$, the discordance between the increasing amplitudes of $[\delta_{p_f}]$ and $[\delta_{p_s}]$ (Fig. 5) and the decreasing amplitude ΔI_{BKCa} (Fig. 7) is symbolized as desynchronization effects for this pathway. This inference can also be deduced from another discordance between $\Delta I_{BKCa}/\bar{I}_{BKCa} \sim 1.5\%$ and $\delta_{p_f}/\bar{p}_f = \delta_{p_s}/\bar{p}_s \sim 19\%$ at $[K]_e = 35.8$ mM.

On the basis of these eigenfunction analyses, we further investigate how synchronizing timings among signal pathways differentiates the spontaneous and agonist-dependent calcium oscillation. For simplicity, we categorize time flows of signal-

ing pathways into two streams: one stream for the cycle of cytosol ions, and the other stream for the cycle of intracellular store. Figure 9 depicts the schematic sketch of coupled time flows of signaling pathways for (a) spontaneous calcium oscillation and (b) agonist-dependent calcium oscillation on the control condition. The curves show the timings of maximum values of ionic concentrations $\delta_{vi \in \{1...6\}}$ and membrane potential $\delta_{vi \in \{7\}}$. The positions of the arrows schedule the time when the maximal amplitudes of current variations occur, and the lengths of the arrows indicate the oscillation amplitudes of channel currents. Arrows are colored as relevant ions. The opposite-direction current variations occur after a time lag $T_{period}/2 = \pi/\omega_{22,i}$ and are not shown here. For the fast decaying spontaneous calcium and long-lasting agonist-dependent calcium oscillation at $[K]_e = 35.8$ mM, we find that (i) the cycle of cytosol ions through transmembrane
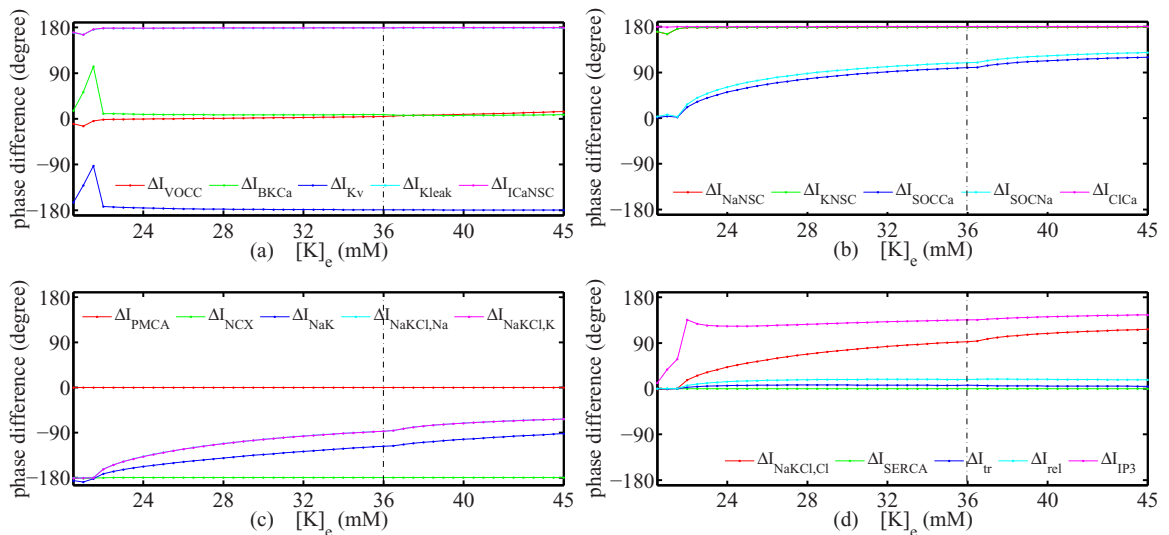

FIG. 8. Phase lag regarding oscillations for current ΔI_i in eigenmode (22,23) versus extracellular potassium concentrations, in which $[\delta_{Ca}]_i = 2 \times 10^{-5}$ mM.
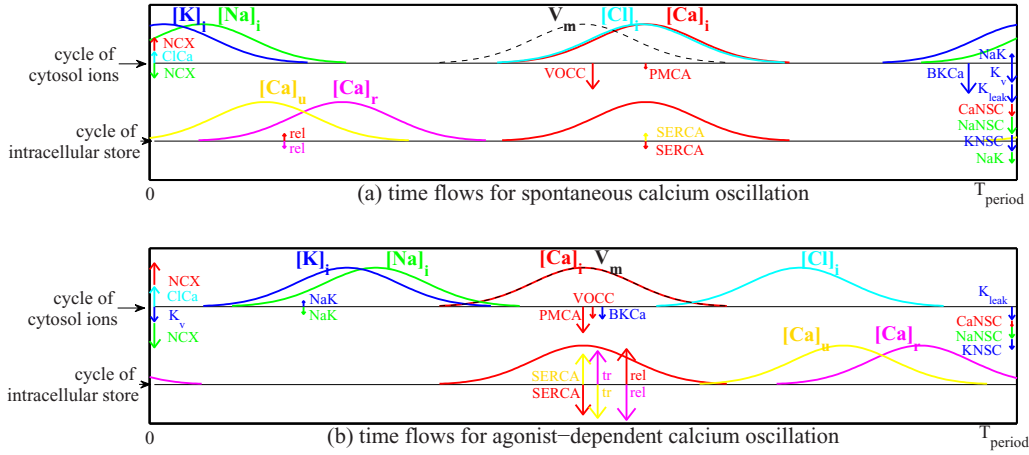
FIG. 9. Schematic sketch of coupled time flows of signaling pathways for (a) spontaneous calcium oscillation and (b) agonist-dependent calcium oscillation. The curves show the timings of the maximum values of ionic concentrations $\delta_{vi \in \{1..6\}}$ and membrane potential $\delta_{vi \in \{7\}}$. The positions of the arrows schedule the time when the maximal amplitudes of current variations occur, and the lengths of the arrows indicate the oscillation amplitudes of channel currents. Arrows are colored as relevant ions. The opposite-direction current variations occur after a time lag $T_{period}/2 = \pi/\omega_{22,i}$ and are not shown here. It is emphasized that the positive and negative arrows represent the relatively increasing and decreasing concentration to the values in equilibrium, respectively, and not the absolute values of concentrations.

currents is dominant in the former condition, while the cycle of intracellular store is dominant in the latter condition; (ii) the time lag between calcium and voltage oscillations is finite in the former condition, while the oscillating phases of calcium and voltage oscillations are exactly synchronous in the latter condition; (iii) aside from the Ca^{2+} itself, K^+ oscillation plays the primary role in the former condition, while Na^+ and Cl^- oscillations are relatively intense in the latter condition. All these findings above interpret the significance of synchronizing timings for vasomotions on different conditions [7,9], and conclude with inevitable involvements of Na^+, K^+, Cl^- ions as well as other relevant channels [43–45].

We also append time-domain calculations corresponding to analyses in Fig. 9(b) to validate our algorithms. Figure 10 shows the time-lag cross-correlation between calcium oscillation $[\delta_{Ca}]_i$ and current oscillations ΔI_i. Figure 11 illustrates the time-lag cross-correlation between calcium oscillation $[\delta_{Ca}]_i$

and other transient variables δ_{vi}. With the given oscillation period of 24 s on the control condition, for instance, the 8 s time lag for ΔI_{NaK} in Fig. 10(c) is equivalent to the shift $-(8/24)T_{period}$ of ΔI_{NaK} from $[Ca]_i$ in Fig. 9(b).

Before studying multiple SMCs, we consider an example of two coupled SMCs (cells I and II), including intracellular and intercellular (see the next section) calcium dynamics, for synchronizing and resonance effects. Extra parameters for the 2-SMCs are defined for inhomogeneous cell volumes, with $vol_I = 1.6$ pℓ and $vol_{II} = 1.1$ pℓ. A numerical calculation of frequency-domain algorithm gives three sets of complex-conjugate eigenvalues for the 2-SMCs: (i) mode S with $\omega_S = -0.028 \pm 0.011i$, (ii) mode A with $\omega_A = -4.96e - 07 \pm 2.46e - 04i$, and (iii) mode B with $\omega_B = -1.49e - 05 \pm 1.98e - 04i$. Mode S is responsible for the spontaneous calcium oscillation, and modes A and B present two kinds of globally agonist-dependent calcium oscillations. Figures 12
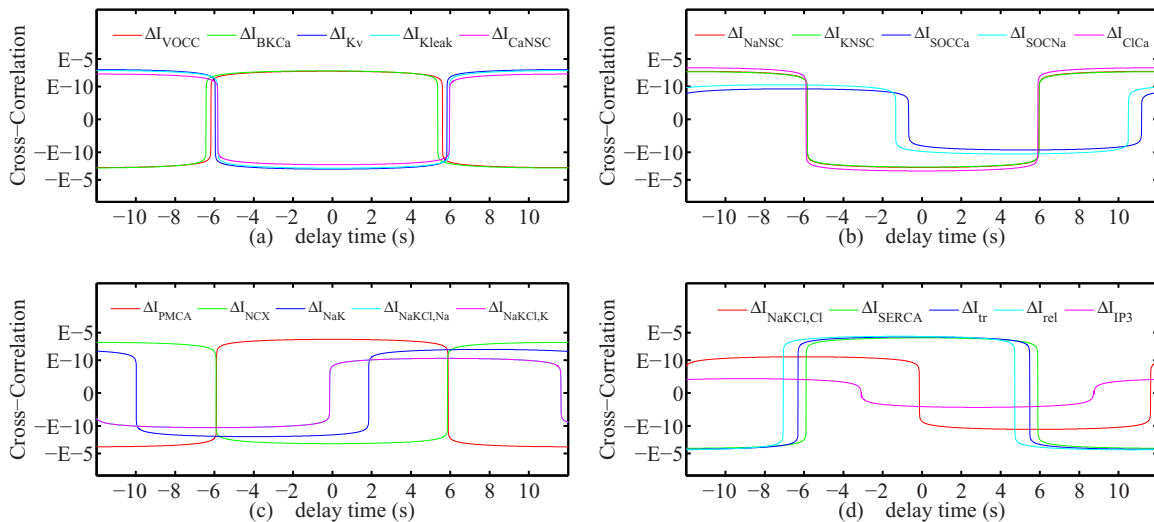

FIG. 10. Time-lag cross-correlation between calcium oscillation $[\delta_{Ca}]_i$ and current oscillations ΔI_i.
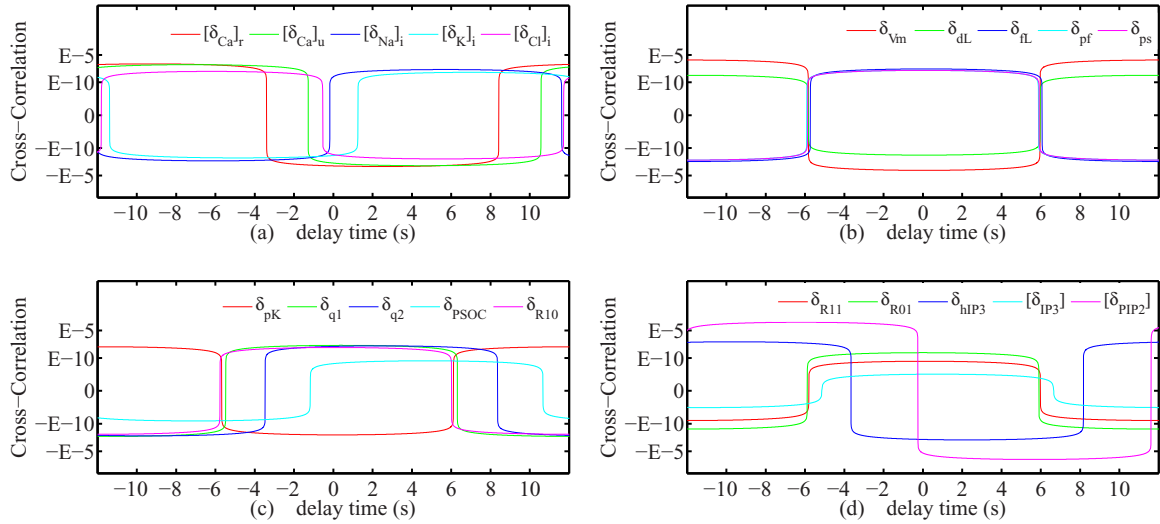
FIG. 11. Time-lag cross-correlation between calcium oscillation $[\delta_{Ca}]_i$ and other transient variables δ_{vi}.

and 13 show the schematic sketch of time flows of signaling pathways for mode A and B, respectively. One can refer to Fig. 9 for the definitions of the curves and arrows. For mode A in Fig. 12, we observe that cell II shows more prevailing calcium oscillation than cell I, while the oscillating phases of calcium and voltage are synchronous in cell II but have a time lag in cell I. Oppositely for mode B in Fig. 13, we observed that cell I shows more prevailing calcium oscillation than cell II, while the oscillating phases of calcium and voltage are almost synchronous in cell I but have a time lag in cell II. We notice that oscillations of voltage in both cells always remain exactly synchronous in the studied cases.

To explore the influences of synchronizing timings, we further carry out time-domain calculations to study 2-SMCs' responses to the external signal, delivered from nerve activity or blood flow, for example [32]. With mode A, we consider three kinds of cyclic calcium stimulations (with frequency ω) to cell I: (a) on-resonance condition with $\omega = \omega_{A,i}$, (b) near-resonance condition with $\omega = 0.9\omega_{A,i}$, and (c) off-resonance condition with $\omega = 10\omega_{A,i}$ as in Fig. 14. Figure 14 shows time evolutions of $[Ca]_i$ and V_m for cells I and II in these

conditions. For the on-resonance condition, the stimulation signals in cell I transfer through gap junction to cell II, and bring both cells into calcium oscillation at mode A; otherwise, the oscillating amplitudes in cell II are more intense than those in cell I, and the oscillating phase of $[Ca]_i$ in cell I has a time lag ($\sim T_{period}/5$) to V_m, agreeing with that in Fig. 12. For the near-resonance condition, the stimulation signals from cell I dissipate during transference, and cell II exhibits incomplete synchronization with cell I. During the period of in-phase oscillations, the oscillating amplitude of $[Ca]_i$ in cell II is strong. During the period of out-phase oscillations, however, the oscillating amplitude of $[Ca]_i$ in cell II is relatively weak. The time lags among $[Ca]_i$ of cell II and the other three variables vary with time. For the off-resonance condition, the stimulation signals from cell I are mostly blocked from cell II. Calcium and voltage oscillations are not observed in cell II, and are significantly suppressed in cell I. With this case of 2-SMCs, we conclude that two factors are essential for efficient signaling communications among cells: (i) correct synchronizing timings among signal pathways occur in SMCs, i.e., the existence of oscillating eigenmodes, and (ii) stimulation signals having
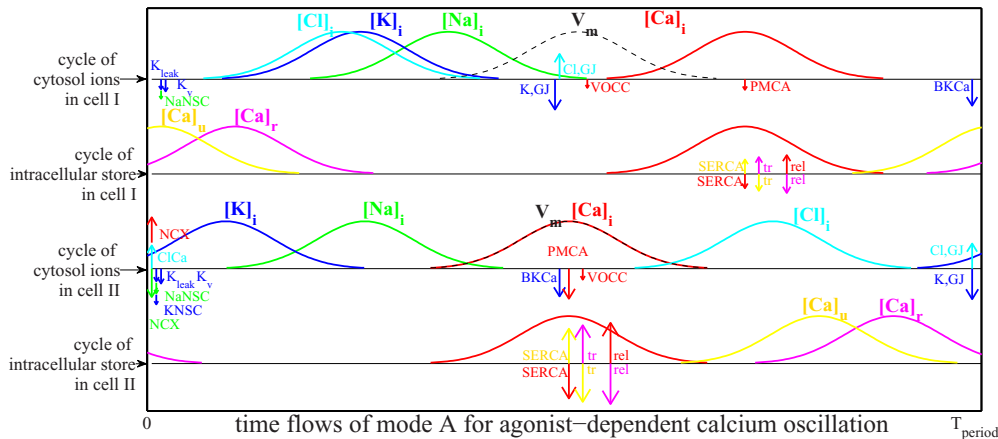

FIG. 12. Schematic sketch of coupled time flows of signaling pathways for eigenmode A, with $T_{period} = 2\pi/\omega_{A,i}$. Relevant definitions for the curves and arrows are similar to those in Fig. 9.

FIG. 13. Schematic sketch of coupled time flows of signaling pathways for eigenmode B, with $T_{period} = 2\pi/\omega_{B,i}$. Relevant definitions for the curves and arrows are similar to those in Fig. 9.
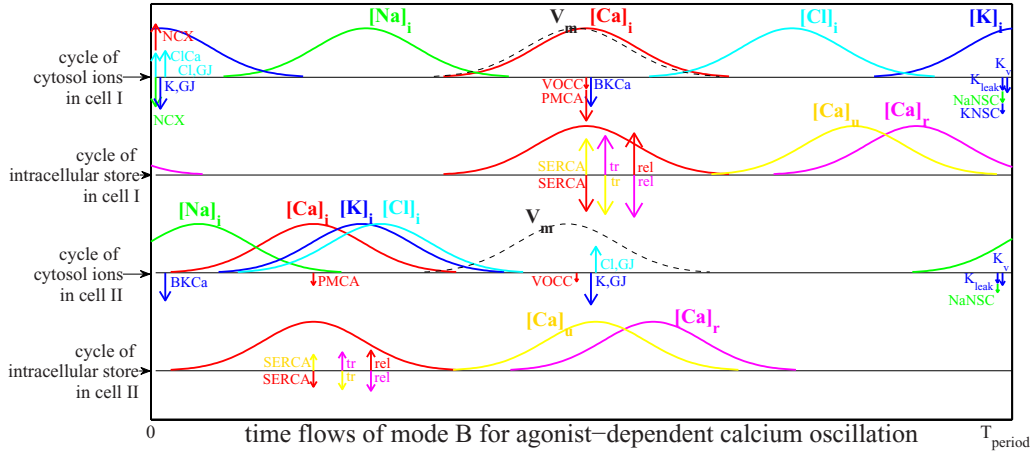
similar frequency to the eigenmode. On the basis of synchronizing and resonance concepts, we investigate functionalities of SMCs' rhythm for practical cell clusters in the next section.

C. Frequency-domain analysis for finite SMC clusters

We now explore physiological functionalities of SMCs' rhythmic oscillations, especially for signaling communications among cells. For intercellular communication, we include the electrodiffusion coupling [23], which uses the Goldman-Hodgkin-Katz (GHK) equation for ionic currents through the gap junctions. These ionic currents were added to the membrane potential equation and corresponding ionic flux equations as in Appendices B 12, D, and F. We assume permeability to be the same for all ions. Gap junction resistance values from experiments were used to calculate the permeability [46]; otherwise, 15% variations of SMC

volumes, as indicated in Ref. [47], were introduced to realize the inhomogeneity of cells.

Figure 15 shows the frequency spectrum for homogeneous 1D clusters at varying cell numbers. Every cell is set in the control condition (except for $[K]_e = 34.8$ mM), and only neighbor cells establish gap junctions. As indicated by green (spontaneous oscillating mode) and red (agonist-dependent oscillating mode) lines in Fig. 15, the oscillation level gradually evolves into a spread band along with increasing cell numbers. This fact infers that a broader-range timing or synchronization among cells is acceptable for rhythmical oscillations in longer clusters. Moreover, properties of red curves in Fig. 15(a) suggest that, due to including more interactions among cells, more transient growing states (positive frequency values) are excited, resulting in the prolongation of duration periods of vasomotions. With an input of delta-function calcium pulse in this resonance medium, we observe functionalities of SMCs' rhythmic oscillations by time-domain calculations.
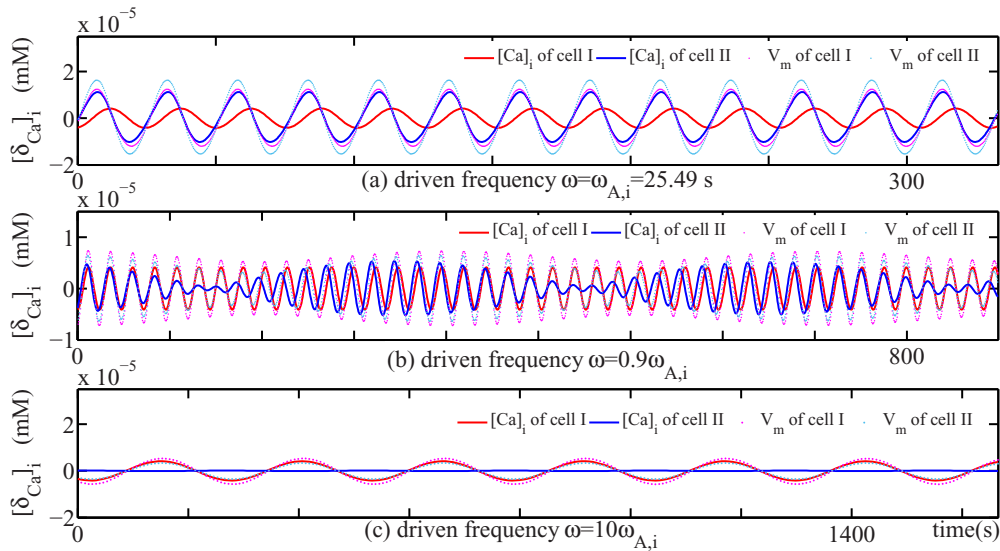

FIG. 14. Time evolutions of $[Ca]_i$ and V_m for two coupled SMCs (I and II) at (a) on-resonance, (b) near-resonance, and (c) off-resonance conditions. Note that all voltage values are scaled and shifted to be comparable with calcium values.
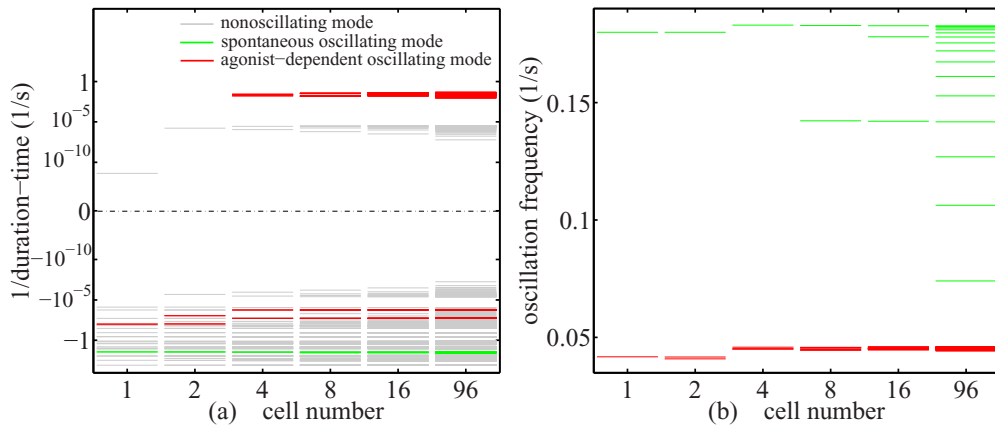
FIG. 15. Frequency spectrum of homogeneous SMC clusters at different cell numbers: (a) real parts of eigenvalues related to growing or decaying time, (b) imaginary parts of eigenvalues related to oscillation periods.

As illustrated in Fig. 16(a), with the same modeling parameters for Fig. 15, the temporal changes of $[Ca^{2+}]_i$ of a 6-SMC cluster are evaluated. In this case, $[K]_e$ is reduced to be 34.6 mM (oscillation activation; see Fig. 4) so as to initially prepare in-equilibrium cells. Another 6-SMC cluster, with $[K]_e = 20$ mM (oscillation-deactivation; see Fig. 4) is computed in Fig. 16(b). Before calcium-pulse stimulation both 6-SMC clusters remain in equilibrium and are indistinguishable by observations. With the given stimulation (suddenly raising the calcium concentration on SMC1 by 35%), the cluster under the oscillation activation first arouses significant calcium peaking by transient resonance in SMC1 [48] [see Fig. 16(a)], and continuously brings calcium signaling toward other SMCs. Numerical results (not shown in the figure) indicate that calcium peaking arises from the activation of ryanodine receptors, which cause $[Ca^{2+}]_i$ to be released from the sarcoplasmic reticulum of cell I. For the cluster under oscillation deactivation in Fig. 16(b), the stimulation from SMC1 dissipates fast and no signaling communications among cells occur, conforming with the observation in experiments of rat mesenteric arterioles [49].

We next include the inhomogeneity of SMCs for biological complexity. Here, 15% stochastic variations of SMC volumes [47] are introduced. Figure 17(a) depicts similar properties on the agonist-dependent oscillating modes (red lines), although the growing mode seems to be more easily excited due to the fluctuation of cell volumes. It is noted that the spontaneous oscillating modes (green lines) remain relatively insensitive to cell number as well as cell uniformity. Figure 17(b) exhibits a broader but less dense level spectrum, versus Fig. 15(b). This fact could imply that the vasomotion in inhomogeneous clusters can decay faster than that in homogeneous ones due to less-overlapping oscillating levels.

We carry out time-domain analysis to study the influences of cell uniformity. Figure 18(a) presents one inhomogeneous 6-SMC cluster with oscillation activation (region II in Fig. 4), while Fig. 18(b) helps analyze another inhomogeneous cluster with oscillation deactivation (region I in Fig. 4). In the case of Fig. 18(a), $[K]_e$ is set to be 35.0 mM in preparation for the initial in-equilibrium cells. In the case of Fig. 18(b), $[K]_e$ is reduced to be 20 mM to achieve the oscillation-deactivation condition. For the oscillation-deactivation condition, the stimulation from SMC1 dissipates fast and no signal communications among cells occur. For the oscillation-activation condition, we find that the signaling transference in inhomogeneous clusters decays relatively faster than that

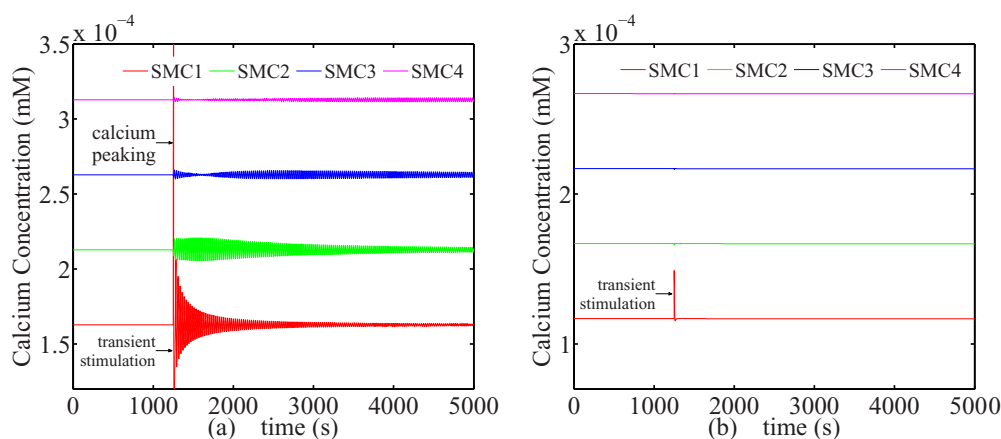FIG. 16. Calcium responses against delta-function calcium stimulation to SMC1 for homogeneous 6-SMCs: (a) at $[K]_e = 34.6$ (oscillation activation; see region II in Fig. 4), and (b) at $[K]_e = 20.0$ (oscillation deactivation; see region I in Fig. 4).
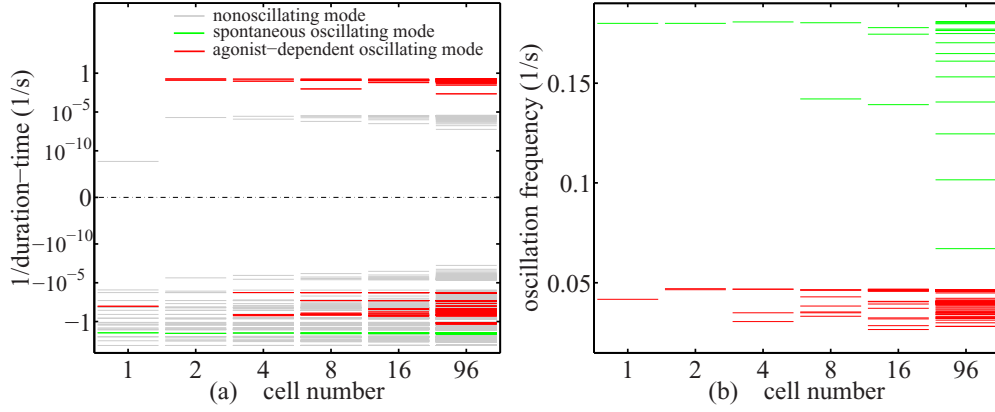
FIG. 17. Frequency spectrum of inhomogeneous SMC clusters at different cell numbers: (a) real parts of eigenvalues related to growing or decaying time, (b) imaginary parts of eigenvalues related to oscillation periods.

in homogeneous ones; otherwise, the signaling delivery among cells presents properties differing from the molecular diffusions and characterizes a frog-leap manner (from SMC1 to SMC3), depending on the specific inhomogeneity. Our calculations explain the observations in the literature [14,16].

IV. CONCLUSION

We have developed herein a detailed biophysical algorithm that intuitionally investigates characteristics of rhythmicity and synchronization related calcium regulation in SMC. Implemented with frequency-domain and time-domain analyses for a single cell, this work recognizes the inherent properties of rhythmical calcium oscillations and validates the utilizations of the eigensystem formulation. In the case of finite SMC clusters, we study the influences of synchronization and resonance conditions, and look at functionalities of cell rhythmicity, calcium peaking, and calcium waves. Relevant calculations offer information underlying the present experimental observations found in the literature. In the future, accompanied by abundant pathological data, this approach could pave an alternate avenue toward physiological and pathological determinations.

APPENDIX A: COMMON VARIABLES

1. Standard parameter values and definitions

$$z_K = 1, \quad z_{Na} = 1, \quad z_{Ca} = 2,$$
$$z_{Cl} = -1, \quad N_{Av} = 6.022 \times 10^{23},$$
$$R = 8341.47 \text{ mJ/molK}, \quad F = 96\,485.34 \text{ C/mol},$$
$$T = 293.0 \text{ K}, \quad C_m = 25 \text{ pF}, \quad A_m = 10^{-6}C_m \text{ cm}^2,$$
$$[Ca]_e = 2.0 \text{ mM}, \quad [Na]_e = 140.0 \text{ mM},$$
$$[K]_e = 5.0 \text{ mM}, \quad [Cl]_e = 129.0 \text{ mM},$$
$$vol_i = 1 \text{ p}\ell, \quad vol_{Ca} = 0.7 \text{ p}\ell,$$
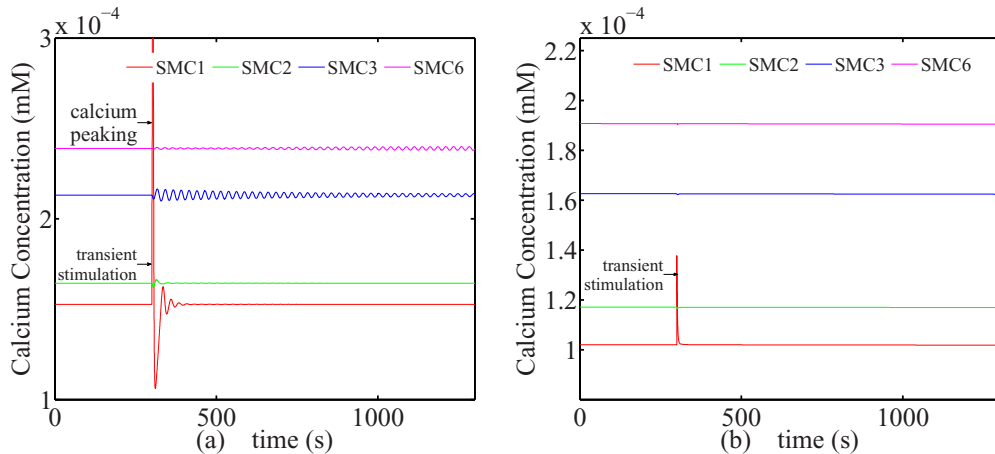$$vol_{SRu} = 0.07 \text{ p}\ell, \quad vol_{SRr} = 0.007 \text{ p}\ell.$$

FIG. 18. Calcium responses against delta-function calcium stimulation to SMC1 for inhomogeneous 6-SMCs: (a) at $[K]_e = 35.0$ (oscillation activation; see region II in Fig. 4), and (b) at $[K]_e = 20.0$ (oscillation deactivation; see region I in Fig. 4).

On the quasiequilibrium condition, the ionic concentrations that we are interested in can be expressed by a time-independent constant term plus a time-dependent fluctuation:

$$[\text{Ca}]_i = [\overline{\text{Ca}}]_i + [\delta_{\text{Ca}}]_i, \quad [\text{Ca}]_r = [\overline{\text{Ca}}]_r + [\delta_{\text{Ca}}]_r,$$

$$[\text{Ca}]_u = [\overline{\text{Ca}}]_u + [\delta_{\text{Ca}}]_u, \quad [\text{Na}]_i = [\overline{\text{Na}}]_i + [\delta_{\text{Na}}]_i,$$

$$[\text{K}]_i = [\overline{\text{K}}]_i + [\delta_{\text{K}}]_i, \quad [\text{Cl}]_i = [\overline{\text{Cl}}]_i + [\delta_{\text{Cl}}]_i,$$

$$V_m = \overline{V}_m + \delta_{V_m}.$$

Herein, $\overline{X}$ represents the equilibrium average constant of X and δ_X represents the deviation from the equilibrium. Similar representations are adopted for variables involved in transient processes, including d_L, f_L, p_f, p_s, p_K, q_1, q_2, P_{SOC}, R_{10}, R_{11}, R_{01}, h_{IP3}, $[R_G^S]$, $[R_{P,G}^S]$, $[G]$, $[\text{IP}_3]$, $[\text{PIP}_2]$, V_{cGMP}, and $[\text{cGMP}]$, and they are introduced in the relevant paragraphs below. Relevant mathematical equations [22], e.g., reversal potentials for ion X, can hence be obtained by using the Taylor series expansion to the first order of fluctuation δ_X at equilibrium:

$$E_X \simeq \frac{RT}{z_X F} \ln([X]_e/[\overline{X}]_i) - \frac{RT}{z_X F} \frac{[\delta_X]_i}{[\overline{X}]_i} \equiv \overline{E}_X + \delta E_X.$$
$$\text{(A1)}$$

Herein, we take $X \in \{\text{Ca}, \text{Na}, \text{K}, \text{Cl}\}$ for example.

2. Initial values of variables

$$[\text{Ca}]_i = 68.0 \times 10^{-6} \text{ mM},$$

$$[\text{Ca}]_r = 0.57 \text{ mM}, \quad [\text{Ca}]_u = 0.66 \text{ mM},$$

$$[\text{Na}]_i = 8.4 \text{ mM}, \quad [\text{K}]_i = 140.0 \text{ mM},$$

$$[\text{Cl}]_i = 59.4 \text{ mM}, \quad V_m = -59.4 \text{ mV},$$

$$[\text{cGMP}] = 0.0 \text{ mM}, \quad [\text{IP}_3] = 0.0 \text{ mM},$$

$$C_m = 25 \text{ pF}, \quad A_m = C_m \times 10^{-6} \text{ cm}^2,$$

$$[\text{NO}] = 10^{-5} \text{ mM, constant,}$$

$$[\text{NE}] = 2 \times 10^{-4} \text{ mM, constant,}$$

$$d_L = d_{L0}, \quad f_L = f_{L0},$$

$$R_{\text{cGMP}} = \frac{[\text{cGMP}]^2}{[\text{cGMP}]^2 + (0.55 \times 10^{-3} \text{ mM})^2},$$

$$p_f = p_s = \overline{p}_o,$$

$$p_K = p_{Ko}, \quad q_1 = q_2 = q_0,$$

$$p_{\text{SOC}} = 0.0, \quad R_{10} = 0.0033,$$

$$R_{11} = 0.000004, \quad R_{01} = 0.9955,$$

$$h_{\text{IP3}} = K_{\text{inh,IP3}}/([\text{Ca}]_i + K_{\text{inh,IP3}}),$$

$$[R_{P,G}^S] = 0, \quad [R_G^S] = [R_{T,G}]\xi_G,$$

$$[\text{PIP}_2] = [\text{PIP}_{2,T}] - (1 + k_{\deg,G}/r_{r,G})\gamma_G[\text{IP}_3],$$

$$r_{h,G0} = k_{\deg,G}\gamma_G[\text{IP}_3]/[\text{PIP}_2],$$

$$[G] = r_{h,G0}(K_{c,G} + [\text{Ca}]_i)/(\alpha_G[\text{Ca}]_i),$$

$$V_{\text{cGMP}} = 0.0.$$

APPENDIX B: MATHEMATICAL MODEL EQUATIONS FOR MEMBRANE ELECTROPHYSIOLOGY

1. L-type voltage-operated Ca²⁺ channels

$$I_{\text{VOCC}} = 10^6 A_m P_{\text{VOCC}} d_L f_L V_m \frac{z_{\text{Ca}}^2 F^2}{RT}$$

$$\times \frac{[\text{Ca}]_e - [\text{Ca}]_i e^{V_m z_{\text{Ca}} F/(RT)}}{1 - e^{V_m z_{\text{Ca}} F/(RT)}} \text{ [pA]}$$

$$\simeq \overline{I}_{\text{VOCC}} + \Delta I_{\text{VOCC}}^{V_m} \delta_{V_m} + \Delta I_{\text{VOCC}}^{\text{Ca}_i}[\delta_{\text{Ca}}]_i$$

$$+ \Delta I_{\text{VOCC}}^{d_L} \delta_{d_L} + \Delta I_{\text{VOCC}}^{f_L} \delta_{f_L}, \quad \text{(B1)}$$

$$\frac{dd_L}{dt} = \frac{d_{L0} - d_L}{\tau_{d_L}} \simeq \frac{d\delta_{d_L}}{dt} \equiv \Delta_{d_L}^{V_m} \delta_{V_m} + \Delta_{d_L}^{d_L} \delta_{d_L}, \quad \text{(B2)}$$

$$\frac{df_L}{dt} = \frac{f_{L0} - f_L}{\tau_{f_L}} \simeq \frac{d\delta_{f_L}}{dt} \equiv \Delta_{f_L}^{V_m} \delta_{V_m} + \Delta_{f_L}^{f_L} \delta_{f_L}, \quad \text{(B3)}$$

on quasiequilibrium conditions (i.e., $dd_L/dt = d\overline{d}_L/dt + d\delta_{d_L}/dt \simeq d\delta_{d_L}/dt$; $df_L/dt = d\overline{f}_L/dt + d\delta_{f_L}/dt \simeq d\delta_{f_L}/dt$) with relevant variables

$$P_{\text{VOCC}} = 1.88 \times 10^{-5} \text{ cm/s},$$

$$d_{L0} = [1 + e^{-V_m/8.3 \text{ mV}}]^{-1}, \quad \text{(B4)}$$

$$f_{L0} = [1 + e^{(V_m+42.0 \text{ mV})/9.1 \text{ mV}}]^{-1}, \quad \text{(B5)}$$

$$\tau_{d_L} = 2.5 e^{-(V_m+40 \text{ mV})^2/(30 \text{ mV})^2} + 1.15 \text{ ms}, \quad \text{(B6)}$$

$$\tau_{f_L} = 65 e^{-(V_m+35 \text{ mV})^2/(25 \text{ mV})^2} + 45 \text{ ms}, \quad \text{(B7)}$$

and the fluctuation terms

$$\Delta I_{\text{VOCC}}^{V_m} = 10^6 \frac{A_m P_{\text{VOCC}} z_{\text{Ca}}^2 F^2}{RT}$$

$$\times \left[\frac{\alpha_1}{\beta_1} + \frac{([\text{Ca}]_e - [\overline{\text{Ca}}]_i)\gamma_1 \overline{V}_m z_{\text{Ca}} F}{\beta_1[1 - \gamma_1]RT} \right], \quad \text{(B8)}$$

$$\Delta I_{\text{VOCC}}^{\text{Ca}_i} = -10^6 \frac{A_m P_{\text{VOCC}} z_{\text{Ca}}^2 F^2}{RT} \frac{\overline{V}_m \gamma_1}{\beta_1}, \quad \text{(B9)}$$

$$\Delta I_{\text{VOCC}}^{d_L} = 10^6 \frac{A_m P_{\text{VOCC}} z_{\text{Ca}}^2 F^2}{RT} \frac{\alpha_1 \overline{V}_m}{\beta_1}[1 + e^{-\overline{V}_m/8.3}], \quad \text{(B10)}$$

$$\Delta I_{\text{VOCC}}^{f_L} = 10^6 \frac{A_m P_{\text{VOCC}} z_{\text{Ca}}^2 F^2}{RT} \frac{\alpha_1 \overline{V}_m}{\beta_1}[1 + e^{(\overline{V}_m+42)/9.1}],$$
$$\text{(B11)}$$

$$\Delta_{d_L}^{V_m} = \frac{e^{-\overline{V}_m/8.3}}{8.3\eta_1(1 + e^{-\overline{V}_m/8.3})^2}, \quad \text{(B12)}$$

$$\Delta_{d_L}^{d_L} = -\frac{1}{\eta_1}, \quad \text{(B13)}$$

$$\Delta_{f_L}^{V_m} = -\frac{e^{(\overline{V}_m+42)/9.1}}{9.1\kappa_1[1 + e^{(\overline{V}_m+42)/9.1}]^2}, \quad \text{(B14)}$$

$$\Delta_{f_L}^{f_L} = -\frac{1}{\kappa_1}. \quad \text{(B15)}$$

Herein,

$$\alpha_1 = [\text{Ca}]_e - [\overline{\text{Ca}}]_i e^{\overline{V}_m z_{\text{Ca}} F/(RT)}, \quad \text{(B16)}$$

$$\beta_1 = [1 + e^{-\overline{V}_m/8.3}][1 + e^{(\overline{V}_m+42)/9.1}][1 - e^{\overline{V}_m z_{Ca} F/(RT)}], \tag{B17}$$

$$\gamma_1 = e^{\overline{V}_m z_{Ca} F/(RT)}, \tag{B18}$$

$$\eta_1 = 2.5 e^{-(\overline{V}_m+40)^2/(30)^2} + 1.15, \tag{B19}$$

$$\kappa_1 = 65 e^{-(\overline{V}_m+35)^2/(25)^2} + 45. \tag{B20}$$

2. Large conductance Ca²⁺-activated K⁺ channels

$$
\begin{aligned}
I_{BKCa} &= A_m N_{BKCa} P_{KCa} i_{KCa} \quad [\text{pA}] \\
&\simeq \overline{I}_{BKCa} + \Delta I_{BKCa}^{V_m} \delta_{V_m} + \Delta I_{BKCa}^{K_i}[\delta_K]_i \\
&\quad + \Delta I_{BKCa}^{p_f} \delta_{p_f} + \Delta I_{BKCa}^{p_s} \delta_{p_s},
\end{aligned} \tag{B21}
$$

$$
\begin{aligned}
\frac{dp_f}{dt} &= \frac{\overline{p}_o - p_f}{\tau_{p_f}} \simeq \frac{d\delta_{p_f}}{dt} \equiv \Delta_{p_f}^{cGMP}[\delta_{cGMP}] \\
&\quad + \Delta_{p_f}^{V_m} \delta_{V_m} + \Delta_{p_f}^{p_f} \delta_{p_f} + \Delta_{p_f}^{Cai}[\delta_{Ca}]_i,
\end{aligned} \tag{B22}
$$

$$
\begin{aligned}
\frac{dp_s}{dt} &= \frac{\overline{p}_o - p_s}{\tau_{p_s}} \simeq \frac{d\delta_{p_s}}{dt} \equiv \Delta_{p_s}^{cGMP}[\delta_{cGMP}] \\
&\quad + \Delta_{p_s}^{V_m} \delta_{V_m} + \Delta_{p_s}^{p_s} \delta_{p_s} + \Delta_{p_s}^{Cai}[\delta_{Ca}]_i,
\end{aligned} \tag{B23}
$$

on quasiequilibrium conditions (i.e., $dp_f/dt = d\overline{p}_f/dt + d\delta_{p_f}/dt \simeq d\delta_{p_f}/dt$; $dp_s/dt = d\overline{p}_s/dt + d\delta_{p_s}/dt \simeq d\delta_{p_s}/dt$) with relevant variables

$$N_{BKCa} = 6.6 \times 10^6 \; 1/\text{cm}^2,$$

$$P_{BKCa} = 3.9 \times 10^{-13} \; \text{cm}^3/\text{s},$$

$$\tau_{p_f} = 0.84 \; \text{ms}, \quad \tau_{p_s} = 35.9 \; \text{ms}, \tag{B24}$$

$$dV_{1/2KCaNO} = 46.3 \; \text{mV}, \quad dV_{1/2KCacGMP} = 76 \; \text{mV},$$

$$\overline{p}_o = \left[1 + e^{-\frac{V_m - V_{1/2KCa}}{18.25 \, \text{mV}}}\right]^{-1},$$

$$P_{KCa} = 0.17 p_f + 0.83 p_s, \tag{B25}$$

$$
\begin{aligned}
V_{1/2KCa} &= -41.7 \log_{10}([\text{Ca}]_i) - dV_{1/2KCaNO} R_{NO} \\
&\quad - dV_{1/2KCacGMP} R_{cGMP} - 128.2,
\end{aligned} \tag{B26}
$$

$$R_{NO} = \frac{[\text{NO}]}{[\text{NO}] + 2 \times 10^{-4} \, \text{mM}}, \tag{B27}$$

$$R_{cGMP} = \frac{[\text{cGMP}]^2}{[\text{cGMP}]^2 + (1.5 \times 10^{-3} \, \text{mM})^2}, \tag{B28}$$

$$i_{KCa} = 10^6 P_{BKCa} V_m \frac{F^2}{RT} \frac{[\text{K}]_e - [\text{K}]_i e^{V_m F/(RT)}}{1 - e^{V_m F/(RT)}}, \tag{B29}$$

and the fluctuation terms

$$
\begin{aligned}
\Delta I_{BKCa}^{V_m} = {}&10^6 \frac{A_m N_{BKCa} P_{BKCa} F^2}{RT} \\
&\times \left[\frac{\gamma_2}{(1 - \alpha_2)(1 + \beta_2)} + \frac{\alpha_2 F \overline{V}_m ([\text{K}]_e - [\overline{\text{K}}]_i)}{(\alpha_2 - 1)^2 (1 + \beta_2) RT}\right],
\end{aligned} \tag{B30}
$$

$$\Delta I_{BKCa}^{K_i} = 10^6 \frac{A_m N_{BKCa} P_{BKCa} F^2}{RT} \frac{\alpha_2 \overline{V}_m}{(\alpha_2 - 1)(1 + \beta_2)}, \tag{B31}$$

$$\Delta I_{BKCa}^{p_f} = 1.7 \times 10^5 \frac{A_m N_{BKCa} P_{BKCa} F^2}{RT} \frac{\gamma_2 \overline{V}_m}{1 - \alpha_2}, \tag{B32}$$

$$\Delta I_{BKCa}^{p_s} = 8.3 \times 10^5 \frac{A_m N_{BKCa} P_{BKCa} F^2}{RT} \frac{\gamma_2 \overline{V}_m}{1 - \alpha_2}, \tag{B33}$$

$$\Delta_{p_f}^{V_m} = \frac{4}{73} \frac{\beta_2}{(1 + \beta_2)^2 \tau_{p_f}}, \tag{B34}$$

$$\Delta_{p_f}^{p_f} = \frac{-1}{\tau_{p_f}}, \tag{B35}$$

$$\Delta_{p_f}^{Cai} = \frac{834}{365 \ln(10)} \frac{\beta_2}{(1 + \beta_2)^2 \tau_{p_f} [\overline{\text{Ca}}]_i}, \tag{B36}$$

$$
\begin{aligned}
\Delta_{p_f}^{cGMP} = {}&\frac{9}{3.65 \times 10^7} \frac{\beta_2}{(1 + \beta_2)^2 \tau_{p_f}} \\
&\times \frac{dV_{1/2KCacGMP}[\overline{\text{cGMP}}]}{([\overline{\text{cGMP}}]^2 + 2.25 \times 10^{-6})^2},
\end{aligned} \tag{B37}
$$

$$\Delta_{p_s}^{V_m} = \frac{4}{73} \frac{\beta_2}{(1 + \beta_2)^2 \tau_{p_s}}, \tag{B38}$$

$$\Delta_{p_s}^{p_s} = \frac{-1}{\tau_{p_s}}, \tag{B39}$$

$$\Delta_{p_s}^{Cai} = \frac{834}{365 \ln(10)} \frac{\beta_2}{(1 + \beta_2)^2 \tau_{p_s} [\overline{\text{Ca}}]_i}, \tag{B40}$$

$$
\begin{aligned}
\Delta_{p_s}^{cGMP} = {}&\frac{9}{3.65 \times 10^7} \frac{\beta_2}{(1 + \beta_2)^2 \tau_{p_s}} \\
&\times \frac{dV_{1/2KCacGMP}[\overline{\text{cGMP}}]}{([\overline{\text{cGMP}}]^2 + 2.25 \times 10^{-6})^2}.
\end{aligned} \tag{B41}
$$

Herein,

$$\alpha_2 = e^{\overline{V}_m F/(RT)}, \tag{B42}$$

$$
\begin{aligned}
\beta_2 = {}&\exp\left[-\frac{4}{73}\overline{V}_m - \frac{166.8}{73} \log_{10}([\overline{\text{Ca}}]_i)\right] \\
&\times \exp\left[-\frac{4}{73}(128.2 + dV_{1/2KCaNO} R_{NO})\right] \\
&\times \exp\left[-\frac{4}{73} dV_{1/2KCacGMP} \times \kappa_2\right],
\end{aligned} \tag{B43}
$$

$$\kappa_2 = \frac{[\overline{\text{cGMP}}]^2}{[\overline{\text{cGMP}}]^2 + (1.5 \times 10^{-3} \, \text{mM})^2}, \tag{B44}$$

$$\gamma_2 = [\text{K}]_e - [\overline{\text{K}}]_i e^{\overline{V}_m F/(RT)}. \tag{B45}$$

3. Voltage-dependent K⁺ channels

$$
\begin{aligned}
I_{Kv} &= g_{Kv} p_K (0.45 q_1 + 0.55 q_2)(V_m - E_K) \quad [\text{pA}] \\
&\simeq \overline{I}_{Kv} + \Delta I_{Kv}^{V_m} \delta_{V_m} + \Delta I_{Kv}^{K_i}[\delta_K]_i \\
&\quad + \Delta I_{Kv}^{p_K} \delta_{p_K} + \Delta I_{Kv}^{q_1} \delta_{q_1} + \Delta I_{Kv}^{q_2} \delta_{q_2},
\end{aligned} \tag{B46}
$$

$$\frac{dp_K}{dt} = \frac{p_{ko} - p_K}{\tau_{p_K}} \simeq \frac{d\delta_{p_K}}{dt} \equiv \Delta_{p_K}^{V_m} \delta_{V_m} + \Delta_{p_K}^{p_K} \delta_{p_K}, \tag{B47}$$

$$\frac{dq_1}{dt} = \frac{q_o - q_1}{\tau_{q_1}} \simeq \frac{d\delta_{q_1}}{dt} \equiv \Delta_{q_1}^{V_m}\delta_{V_m} + \Delta_{q_1}^{q_1}\delta_{q_1}, \quad \text{(B48)}$$

$$\frac{dq_2}{dt} = \frac{q_o - q_2}{\tau_{q_2}} \simeq \frac{d\delta_{q_2}}{dt} \equiv \Delta_{q_2}^{V_m}\delta_{V_m} + \Delta_{q_2}^{q_2}\delta_{q_2}, \quad \text{(B49)}$$

on quasiequilibrium conditions with relevant variables

$$g_{Kv} = 1.35 \text{ nS},$$

$$\tau_{q_1} = 371.0 \text{ ms}, \quad \tau_{q_2} = 2884.0 \text{ ms},$$

$$\tau_{p_K} = 61.5 e^{-0.027 V_m} \text{ ms},$$

$$p_{Ko} = \left[1 + e^{-\frac{V_m + 11 \text{ mV}}{15 \text{ mV}}}\right]^{-1}, \quad \text{(B50)}$$

$$q_o = \left[1 + e^{\frac{V_m + 40 \text{ mV}}{14 \text{ mV}}}\right]^{-1}, \quad \text{(B51)}$$

and the fluctuation terms

$$\Delta I_{Kv}^{V_m} = \frac{g_{Kv}}{(1 + \alpha_3)(1 + \beta_3)}, \quad \text{(B52)}$$

$$\Delta I_{Kv}^{K_i} = \frac{g_{Kv} RT}{[\overline{K}]_i z_K F (1 + \alpha_3)(1 + \beta_3)}, \quad \text{(B53)}$$

$$\Delta I_{Kv}^{p_K} = \frac{g_{Kv}(\overline{V}_m - \overline{E}_K)}{(1 + \beta_3)}, \quad \text{(B54)}$$

$$\Delta I_{Kv}^{q_1} = \frac{9 g_{Kv}(\overline{V}_m - \overline{E}_K)}{20(1 + \alpha_3)}, \quad \text{(B55)}$$

$$\Delta I_{Kv}^{q_2} = \frac{11 g_{Kv}(\overline{V}_m - \overline{E}_K)}{20(1 + \alpha_3)}, \quad \text{(B56)}$$

$$\Delta_{p_K}^{V_m} = \frac{2e^{-\frac{11}{15} - \frac{119}{3000}\overline{V}_m}}{1845(1 + \alpha_3)^2}, \quad \Delta_{p_K}^{p_K} = -\frac{2e^{0.027\overline{V}_m}}{123}, \quad \text{(B57)}$$

$$\Delta_{q_1}^{V_m} = \frac{-\beta_3}{14\tau_{q_1}(1 + \beta_3)^2}, \quad \Delta_{q_1}^{q_1} = \frac{-1}{\tau_{q_1}}, \quad \text{(B58)}$$

$$\Delta_{q_2}^{V_m} = \frac{-\beta_3}{14\tau_{q_2}(1 + \beta_3)^2}, \quad \Delta_{q_2}^{q_2} = \frac{-1}{\tau_{q_2}}. \quad \text{(B59)}$$

Herein,

$$\alpha_3 = e^{\frac{-1}{15}(\overline{V}_m + 11)}, \quad \beta_3 = e^{\frac{1}{14}(\overline{V}_m + 40)}. \quad \text{(B60)}$$

4. Unspecified K$^+$ leak channels

$$I_{Kleak} = g_{Kleak}(V_m - E_K) \text{ [pA]}$$
$$\simeq \overline{I}_{Kleak} + \Delta I_{Kleak}^{V_m}\delta_{V_m} + \Delta I_{Kleak}^{K_i}[\delta_K]_i, \quad \text{(B61)}$$

on quasiequilibrium conditions with relevant variables

$$g_{Kleak} = 0.067 \text{ nS}$$

and the fluctuation terms

$$\Delta I_{Kleak}^{V_m} = g_{Kleak}, \quad \text{(B62)}$$

$$\Delta I_{Kleak}^{K_i} = \frac{g_{Kleak} RT}{[\overline{K}]_i z_K F}. \quad \text{(B63)}$$

5. Nonselective cation channels

$$I_{CaNSC} = 10^6 A_m d_{NSC} P_{oNSC} P_{CaNSC} V_m \frac{z_{Ca}^2 F^2}{RT}$$

$$\times \frac{[Ca]_e - [Ca]_i e^{V_m z_{Ca} F/(RT)}}{1 - e^{V_m z_{Ca} F/(RT)}}$$

$$\simeq \overline{I}_{CaNSC} + \Delta I_{CaNSC}^{V_m}\delta_{V_m} + \Delta I_{CaNSC}^{Ca_i}[\delta_{Ca}]_i, \quad \text{(B64)}$$

$$I_{NaNSC} = 10^6 A_m \left[\frac{[DAG]}{[DAG] + K_{NSC}} + d_{NSC}\right] V_m$$

$$\times \frac{P_{oNSC} P_{NaNSC} F^2}{RT} \frac{[Na]_e - [Na]_i e^{V_m F/(RT)}}{1 - e^{V_m F/(RT)}}$$

$$\simeq \overline{I}_{NaNSC} + \Delta I_{NaNSC}^{V_m}\delta_{V_m} + \Delta I_{NaNSC}^{Na_i}[\delta_{Na}]_i, \quad \text{(B65)}$$

$$I_{KNSC} = 10^6 A_m \left[\frac{[DAG]}{[DAG] + K_{NSC}} + d_{NSC}\right] V_m$$

$$\times \frac{P_{oNSC} P_{KNSC} F^2}{RT} \frac{[K]_e - [K]_i e^{V_m F/(RT)}}{1 - e^{V_m F/(RT)}}$$

$$\simeq \overline{I}_{KNSC} + \Delta I_{KNSC}^{V_m}\delta_{V_m} + \Delta I_{KNSC}^{K_i}[\delta_K]_i, \quad \text{(B66)}$$

on quasiequilibrium conditions with relevant variables

$$d_{NSC} = 0.0244, \quad K_{NSC} = 3 \times 10^{-3} \text{ mM},$$

$$P_{NaNSC} = 5.11 \times 10^{-7} \text{ cm/s},$$

$$[DAG] = [\overline{IP}_3], \quad \text{(B67)}$$

$$P_{KNSC} = 1.06 P_{NaNSC}, \quad P_{CaNSC} = 4.54 P_{NaNSC},$$

$$P_{oNSC} = \frac{0.57}{1 + e^{-\frac{V_m - 47.12 \text{ mV}}{24.24 \text{ mV}}}} + 0.43, \quad \text{(B68)}$$

and the fluctuation terms

$$\Delta I_{CaNSC}^{V_m} = \frac{0.43\eta_5\beta_5 P_{CaNSC}}{1 - \gamma_5^{z_{Ca}}}$$

$$+ \frac{([Ca]_e - [\overline{Ca}]_i)\gamma_5^{z_{Ca}} P_{CaNSC}\beta_5 F \overline{V}_m z_{Ca}}{100(1 - \gamma_5^{z_{Ca}})^2 RT/43}$$

$$+ \frac{0.57\eta_5\beta_5 P_{CaNSC}}{(1 - \gamma_5^{z_{Ca}})(1 + \zeta_5)}$$

$$+ \frac{([Ca]_e - [\overline{Ca}]_i)\gamma_5^{z_{Ca}} P_{CaNSC}\beta_5 F \overline{V}_m z_{Ca}}{100(1 - \gamma_5^{z_{Ca}})^2(1 + \zeta_5)RT/57}$$

$$+ \frac{19\zeta_5\beta_5 P_{CaNSC}\overline{V}_m\eta_5}{808(1 + \zeta_5)^2(1 - \gamma_5^{z_{Ca}})}, \quad \text{(B69)}$$

$$\Delta I_{CaNSC}^{Ca_i} = \frac{\gamma_5^{z_{Ca}} P_{CaNSC}\beta_5 \overline{V}_m}{\gamma_5^{z_{Ca}} - 1}\left(0.43 + \frac{0.57}{1 + \zeta_5}\right), \quad \text{(B70)}$$

$$\Delta I_{NaNSC}^{V_m} = \frac{0.43\lambda_5\alpha_5 P_{NaNSC}}{1 - \gamma_5}$$

$$+ \frac{([Na]_e - [\overline{Na}]_i)\gamma_5 P_{NaNSC}\alpha_5 F \overline{V}_m}{100(1 - \gamma_5)^2 RT/43}$$

$$+ \frac{0.57\lambda_5\alpha_5 P_{NaNSC}}{(1 - \gamma_5)(1 + \zeta_5)}$$

$$+ \frac{([\text{Na}]_e - [\overline{\text{Na}}]_i)\gamma_5 P_{\text{NaNSC}}\alpha_5 F\overline{V}_m}{100(1-\gamma_5)^2(1+\zeta_5)RT/57}$$

$$+ \frac{19\zeta_5\alpha_5 P_{\text{NaNSC}}\overline{V}_m\lambda_5}{808(1+\zeta_5)^2(1-\gamma_5)}, \tag{B71}$$

$$\Delta I_{\text{NaNSC}}^{\text{Na}_i} = \frac{\gamma_5 P_{\text{NaNSC}}\alpha_5\overline{V}_m}{\gamma_5-1}\left(0.43 + \frac{0.57}{1+\zeta_5}\right), \tag{B72}$$

$$\Delta I_{\text{KNSC}}^{V_m} = \frac{0.43\kappa_5\alpha_5 P_{\text{KNSC}}}{1-\gamma_5}$$

$$+ \frac{([\text{K}]_e - [\overline{\text{K}}]_i)\gamma_5 P_{\text{KNSC}}\alpha_5 F\overline{V}_m}{100(1-\gamma_5)^2 RT/43}$$

$$+ \frac{0.57\kappa_5\alpha_5 P_{\text{KNSC}}}{(1-\gamma_5)(1+\zeta_5)}$$

$$+ \frac{([\text{K}]_e - [\overline{\text{K}}]_i)\gamma_5 P_{\text{KNSC}}\alpha_5 F\overline{V}_m}{100(1-\gamma_5)^2(1+\zeta_5)RT/57}$$

$$+ \frac{19\zeta_5\alpha_5 P_{\text{KNSC}}\overline{V}_m\kappa_5}{808(1+\zeta_5)^2(1-\gamma_5)}, \tag{B73}$$

$$\Delta I_{\text{KNSC}}^{\text{K}_i} = \frac{\gamma_5 P_{\text{KNSC}}\alpha_5\overline{V}_m}{\gamma_5-1}\left(0.43 + \frac{0.57}{1+\zeta_5}\right). \tag{B74}$$

Herein,

$$\alpha_5 = \frac{10^6 A_m F^2}{RT}\left[\frac{[\text{DAG}]}{[\text{DAG}]+K_{\text{NSC}}} + d_{\text{NSC}}\right], \tag{B75}$$

$$\beta_5 = 10^6 A_m d_{\text{NSC}}\frac{z_{\text{Ca}}^2 F^2}{RT}, \tag{B76}$$

$$\gamma_5 = e^{\frac{\overline{V}_m F}{RT}}, \quad \zeta_5 = e^{-\frac{\overline{V}_m - 47.12}{24.24}}, \tag{B77}$$

$$\eta_5 = [\text{Ca}]_e - [\overline{\text{Ca}}]_i e^{\overline{V}_m z_{\text{Ca}} F/(RT)}, \tag{B78}$$

$$\lambda_5 = [\text{Na}]_e - [\overline{\text{Na}}]_i e^{\overline{V}_m F/(RT)}, \tag{B79}$$

$$\kappa_5 = [\text{K}]_e - [\overline{\text{K}}]_i e^{\overline{V}_m F/(RT)}. \tag{B80}$$

6. Store-operated nonselective cation channels

$$I_{\text{SOCCa}} = g_{\text{SOCCa}} P_{\text{SOC}}(V_m - E_{\text{Ca}})$$
$$\simeq \overline{I}_{\text{SOCCa}} + \Delta I_{\text{SOCCa}}^{P_{\text{SOC}}}\delta_{P_{\text{SOC}}}$$
$$+ \Delta I_{\text{SOCCa}}^{V_m}\delta_{V_m} + \Delta I_{\text{SOCCa}}^{\text{Ca}_i}[\delta_{\text{Ca}}]_i, \tag{B81}$$

$$I_{\text{SOCNa}} = g_{\text{SOCNa}} P_{\text{SOC}}(V_m - E_{\text{Na}})$$
$$\simeq \overline{I}_{\text{SOCNa}} + \Delta I_{\text{SOCNa}}^{P_{\text{SOC}}}\delta_{P_{\text{SOC}}}$$
$$+ \Delta I_{\text{SOCNa}}^{V_m}\delta_{V_m} + \Delta I_{\text{SOCNa}}^{\text{Na}_i}[\delta_{\text{Na}}]_i, \tag{B82}$$

$$\frac{dp_{\text{SOC}}}{dt} = \frac{p_{\text{SOC},o} - p_{\text{SOC}}}{\tau_{\text{SOC}}} \simeq \frac{d\delta_{p_{\text{SOC}}}}{dt}$$
$$\equiv \Delta_{p_{\text{SOC}}}^{\text{Ca}_u}\delta_{\text{Ca}_u} + \Delta_{p_{\text{SOC}}}^{p_{\text{SOC}}}\delta_{p_{\text{SOC}}}, \tag{B83}$$

on quasiequilibrium conditions with relevant variables

$$g_{\text{SOCCa}} = 0.0083 \text{ nS}, \quad g_{\text{SOCNa}} = 0.0575 \text{ nS},$$
$$\tau_{\text{SOC}} = 100.0 \text{ ms},$$

$$P_{\text{SOC},o} = \left(1 + \frac{[\text{Ca}]_u}{10^{-4} \text{ mM}}\right)^{-1}, \tag{B84}$$

and the fluctuation terms

$$\Delta I_{\text{SOCCa}}^{V_m} = \frac{g_{\text{SOCCa}}}{1 + 10^4[\overline{\text{Ca}}]_u}, \tag{B85}$$

$$\Delta I_{\text{SOCCa}}^{\text{Ca}_i} = \frac{g_{\text{SOCCa}}RT}{[\overline{\text{Ca}}]_i(1 + 10^4[\overline{\text{Ca}}]_u)Fz_{\text{Ca}}}, \tag{B86}$$

$$\Delta I_{\text{SOCCa}}^{P_{\text{SOC}}} = g_{\text{SOCCa}}(\overline{V}_m - \overline{E}_{\text{Ca}}), \tag{B87}$$

$$\Delta I_{\text{SOCNa}}^{V_m} = \frac{g_{\text{SOCNa}}}{1 + 10^4[\overline{\text{Ca}}]_u}, \tag{B88}$$

$$\Delta I_{\text{SOCNa}}^{\text{Na}_i} = \frac{g_{\text{SOCNa}}RT}{[\overline{\text{Na}}]_i(1 + 10^4[\overline{\text{Ca}}]_u)F}, \tag{B89}$$

$$\Delta I_{\text{SOCNa}}^{P_{\text{SOC}}} = g_{\text{SOCNa}}(\overline{V}_m - \overline{E}_{\text{Na}}), \tag{B90}$$

$$\Delta_{p_{\text{SOC}}}^{\text{Ca}_u} = \frac{-10^4\tau_{\text{SOC}}^{-1}}{(1 + 10^4[\overline{\text{Ca}}]_u)^2}, \quad \Delta_{p_{\text{SOC}}}^{p_{\text{SOC}}} = \frac{-1}{\tau_{\text{SOC}}}. \tag{B91}$$

7. Calcium-activated chloride channels

$$I_{\text{ClCa}} = C_m g_{\text{ClCa}} P_{\text{Cl}}(V_m - E_{\text{Cl}}) \text{ [pA]}$$
$$\simeq \overline{I}_{\text{ClCa}} + \Delta I_{\text{ClCa}}^{V_m}\delta_{V_m} + \Delta I_{\text{ClCa}}^{\text{Ca}_i}[\delta_{\text{Ca}}]_i$$
$$+ \Delta I_{\text{ClCa}}^{\text{Cl}_i}[\delta_{\text{Cl}}]_i + \Delta I_{\text{ClCa}}^{\text{cGMP}}[\delta_{\text{cGMP}}], \tag{B92}$$

on quasiequilibrium conditions with relevant variables

$$g_{\text{ClCa}} = 0.23 \text{ nS/pF}, \quad n_{\text{ClcGMP}} = 3.3,$$
$$K_{\text{ClCa}} = 3.65 \times 10^{-4} \text{ mM}, \quad n_{\text{ClCa}} = 2,$$
$$R_{\text{ClcGMP}} = 0.0132,$$
$$K_{\text{ClcGMP}} = 6.4 \times 10^{-3} \text{ mM},$$

$$P_{\text{Cl}} = R_{\text{ClcGMP}}\frac{([\text{Ca}]_i)^{n_{\text{ClCa}}}}{([\text{Ca}]_i)^{n_{\text{ClCa}}} + (K_{\text{ClCa}})^{n_{\text{ClCa}}}}$$
$$+ \alpha_{\text{Cl}}\frac{([\text{Ca}]_i)^{n_{\text{ClCa}}}}{([\text{Ca}]_i)^{n_{\text{ClCa}}} + (K_{\text{ClCa,cGMP}})^{n_{\text{ClCa}}}}, \tag{B93}$$

$$\alpha_{\text{Cl}} = \frac{([\text{cGMP}])^{n_{\text{ClcGMP}}}}{([\text{cGMP}])^{n_{\text{ClcGMP}}} + (K_{\text{ClcGMP}})^{n_{\text{ClcGMP}}}}, \tag{B94}$$

$$K_{\text{ClCa,cGMP}} = (1 - 0.9\alpha_{\text{Cl}}) \times 4 \times 10^{-4} \text{ mM} \tag{B95}$$

and the fluctuation terms

$$\Delta I_{\text{ClCa}}^{V_m} = C_m g_{\text{ClCa}}[\alpha_7 R_{\text{ClcGMP}} + \beta_7\gamma_7], \tag{B96}$$

$$\Delta I_{\text{ClCa}}^{\text{Ca}_i} = C_m g_{\text{ClCa}} n_{\text{ClCa}}(\overline{V}_m - \overline{E}_{\text{Cl}})[\overline{\text{Ca}}]_i^{-n_{\text{ClCa}}-1}$$
$$\times \left[\alpha_7^2 R_{\text{ClcGMP}}(K_{\text{ClCa}})^{n_{\text{ClCa}}} + \beta_7^2\gamma_7\left(\frac{1-0.9\gamma_7}{2500}\right)^{n_{\text{ClCa}}}\right], \tag{B97}$$

$$\Delta I_{\text{ClCa}}^{\text{Cl}_i} = \frac{-C_m g_{\text{ClCa}} RT(\alpha_7 R_{\text{ClcGMP}} + \beta_7 \gamma_7)}{[\overline{\text{Cl}}]_i F}, \quad \text{(B98)}$$

$$\Delta I_{\text{ClCa}}^{\text{cGMP}} = C_m g_{\text{ClCa}} \beta_7^2 n_{\text{ClcGMP}} (\overline{V}_m - \overline{E}_{\text{Cl}})$$

$$\times \left[\frac{\gamma_7^2 (K_{\text{ClcGMP}})^{n_{\text{ClcGMP}}}}{([\overline{\text{cGMP}}])^{1+n_{\text{ClcGMP}}}} \right.$$

$$+ \frac{(K_{\text{ClcGMP}})^{n_{\text{ClcGMP}}} \gamma_7^2 \left(\frac{1-0.9\gamma_7}{2500}\right)^{n_{\text{ClCa}}}}{([\overline{\text{Ca}}]_i)^{n_{\text{ClCa}}} ([\overline{\text{cGMP}}])^{1+n_{\text{ClcGMP}}}}$$

$$\left. + \frac{9 n_{\text{ClCa}} \gamma_7^2 \kappa_7 \left(\frac{1-0.9\gamma_7}{2500}\right)^{n_{\text{ClCa}}}}{([\overline{\text{Ca}}]_i)^{n_{\text{ClCa}}} [\overline{\text{cGMP}}]} \right]. \quad \text{(B99)}$$

Herein,

$$\alpha_7 = \frac{([\overline{\text{Ca}}]_i)^{n_{\text{ClCa}}}}{([\overline{\text{Ca}}]_i)^{n_{\text{ClCa}}} + (K_{\text{ClCa}})^{n_{\text{ClCa}}}}, \quad \text{(B100)}$$

$$\beta_7 = \frac{([\overline{\text{Ca}}]_i)^{n_{\text{ClCa}}}}{([\overline{\text{Ca}}]_i)^{n_{\text{ClCa}}} + \left(\frac{1-0.9\gamma_7}{2500}\right)^{n_{\text{ClCa}}}}, \quad \text{(B101)}$$

$$\gamma_7 = \frac{([\overline{\text{cGMP}}])^{n_{\text{ClcGMP}}}}{([\overline{\text{cGMP}}])^{n_{\text{ClcGMP}}} + (K_{\text{ClcGMP}})^{n_{\text{ClcGMP}}}}, \quad \text{(B102)}$$

$$\kappa_7 = \frac{(K_{\text{ClcGMP}})^{n_{\text{ClcGMP}}}}{([\overline{\text{cGMP}}])^{n_{\text{ClcGMP}}} + 10(K_{\text{ClcGMP}})^{n_{\text{ClcGMP}}}}. \quad \text{(B103)}$$

8. Plasma membrane Ca²⁺ pump

$$I_{\text{PMCA}} = I_{\text{PMCA},0} \frac{[\text{Ca}]_i}{[\text{Ca}]_i + K_{m,\text{PMCA}}}$$

$$\simeq \overline{I}_{\text{PMCA}} + \Delta I_{\text{PMCA}}^{\text{Ca}_i}[\delta_{\text{Ca}}]_i, \quad \text{(B104)}$$

on quasiequilibrium conditions with relevant variables

$$I_{\text{PMCA},0} = 5.37 \text{ pA},$$

$$K_{m,\text{PMCA}} = 1.7 \times 10^{-4} \text{ mM},$$

and the fluctuation terms

$$\Delta I_{\text{PMCA}}^{\text{Ca}_i} = I_{\text{PMCA},0} \frac{K_{m,\text{PMCA}}}{([\overline{\text{Ca}}]_i + K_{m,\text{PMCA}})^2}. \quad \text{(B105)}$$

9. Plasma membrane Na⁺-Ca²⁺ exchange

$$I_{\text{NCX}} = g_{\text{NCX}} R_{\text{NCX,cGMP}}$$

$$\times \frac{[\text{Na}]_i^3 [\text{Ca}]_e \phi_F - [\text{Na}]_e^3 [\text{Ca}]_i \phi_R}{1 + d_{\text{NCX}} ([\text{Na}]_e^3 [\text{Ca}]_i + [\text{Na}]_i^3 [\text{Ca}]_e)}$$

$$\simeq \overline{I}_{\text{NCX}} + \Delta I_{\text{NCX}}^{V_m} \delta_{V_m} + \Delta I_{\text{NCX}}^{\text{Ca}_i}[\delta_{\text{Ca}}]_i$$

$$+ \Delta I_{\text{NCX}}^{\text{Na}_i}[\delta_{\text{Na}}]_i + \Delta I_{\text{NCX}}^{\text{cGMP}}[\delta_{\text{cGMP}}], \quad \text{(B106)}$$

on quasiequilibrium conditions with relevant variables

$$g_{\text{NCX}} = 0.000487 \text{ pA},$$

$$d_{\text{NCX}} = 0.0003, \quad \gamma_{\text{NCX}} = 0.45,$$

$$R_{\text{NCX,cGMP}} = 1 + \frac{0.55[\text{cGMP}]}{[\text{cGMP}] + 0.045 \text{ mM}}, \quad \text{(B107)}$$

$$\phi_F = \exp\left[\frac{\gamma_{\text{NCX}} V_m F}{RT}\right], \quad \text{(B108)}$$

$$\phi_R = \exp\left[\frac{(\gamma_{\text{NCX}} - 1) V_m F}{RT}\right], \quad \text{(B109)}$$

and the fluctuation terms

$$\Delta I_{\text{NCX}}^{V_m} = \frac{\gamma_9 F}{\alpha_9 RT} \left\{ \beta_9^{-1}[\overline{\text{Ca}}]_i [\text{Na}]_e^3 (1 - \gamma_{\text{NCX}}) \right.$$

$$\left. + [\text{Ca}]_e [\overline{\text{Na}}]_i^3 \gamma_{\text{NCX}} \right\}, \quad \text{(B110)}$$

$$\Delta I_{\text{NCX}}^{\text{Ca}_i} = \frac{-\gamma_9}{\alpha_9^2} \left\{ \beta_9^{-1}[\text{Na}]_e^3 + d_{\text{NCX}}[\text{Na}]_e^3 [\text{Ca}]_e [\overline{\text{Na}}]_i^3 \right.$$

$$\left. + d_{\text{NCX}} \beta_9^{-1}[\text{Na}]_e^3 [\text{Ca}]_e [\overline{\text{Na}}]_i^3 \right\}, \quad \text{(B111)}$$

$$\Delta I_{\text{NCX}}^{\text{Na}_i} = \frac{3\gamma_9}{\alpha_9^2} \left\{ d_{\text{NCX}}[\text{Ca}]_e [\overline{\text{Ca}}]_i [\text{Na}]_e^3 [\overline{\text{Na}}]_i^2 \right.$$

$$\left. + \beta_9^{-1} d_{\text{NCX}}[\text{Ca}]_e [\overline{\text{Ca}}]_i [\text{Na}]_e^3 [\overline{\text{Na}}]_i^2 + [\text{Ca}]_e [\overline{\text{Na}}]_i^2 \right\}, \quad \text{(B112)}$$

$$\Delta I_{\text{NCX}}^{\text{cGMP}} = \frac{990 g_{\text{NCX}} \times \beta_9^{\gamma_{\text{NCX}}}}{\alpha_9 (9 + 200[\overline{\text{cGMP}}])^2} \left\{ [\text{Ca}]_e [\overline{\text{Na}}]_i^3 \right.$$

$$\left. - \beta_9^{-1}[\overline{\text{Ca}}]_i [\text{Na}]_e^3 \right\}. \quad \text{(B113)}$$

Herein,

$$\alpha_9 = 1 + d_{\text{NCX}}\left([\text{Na}]_e^3 [\overline{\text{Ca}}]_i + [\overline{\text{Na}}]_i^3 [\text{Ca}]_e\right), \quad \text{(B114)}$$

$$\beta_9 = \exp[\overline{V}_m F/(RT)], \quad \text{(B115)}$$

$$\gamma_9 = g_{\text{NCX}} \times \kappa_9 \exp[\gamma_{\text{NCX}} \overline{V}_m F/(RT)], \quad \text{(B116)}$$

$$\kappa_9 = 1 + \frac{0.55[\overline{\text{cGMP}}]}{[\overline{\text{cGMP}}] + 0.045}. \quad \text{(B117)}$$

10. Sodium-potassium pump

$$I_{\text{NaK}} = C_m I_{\text{NaK},0} Q \frac{[\text{Na}]_i^{n_{H\text{Nai}}}}{[\text{Na}]_i^{n_{H\text{Nai}}} + \text{Na}_{d\text{Nai}}^{n_{H\text{Nai}}}}$$

$$\times \frac{[\text{K}]_e^{n_{H\text{Ke}}}}{[\text{K}]_e^{n_{H\text{Ke}}} + \text{K}_{d\text{Ke}}^{n_{H\text{Ke}}}} \frac{V_m + 150 \text{ mV}}{V_m + 200 \text{ mV}}$$

$$\simeq \overline{I}_{\text{NaK}} + \Delta I_{\text{NaK}}^{V_m} \delta_{V_m} + \Delta I_{\text{NaK}}^{\text{Na}_i}[\delta_{\text{Na}}]_i, \quad \text{(B118)}$$

on quasiequilibrium conditions with relevant variables

$$n_{H\text{Ke}} = 1.1, \quad n_{H\text{Nai}} = 1.7,$$

$$\text{K}_{d\text{Ke}} = 1.6 \text{ mM}, \quad \text{Na}_{d\text{Nai}} = 22 \text{ mM},$$

$$I_{\text{NaK},0} = 2.3083 \text{ pA/pF},$$

$$Q = Q_{10}^{(T-309.15 \text{ K})/(10 \text{ K})}, \quad Q_{10} = 1.87, \quad \text{(B119)}$$

and the fluctuation terms

$$\Delta I_{\text{NaK}}^{V_m} = \frac{50 C_m I_{\text{NaK},0} Q [\text{K}]_e^{n_{H\text{Ke}}} [\overline{\text{Na}}]_i^{n_{H\text{Nai}}}}{\alpha_{10} \beta_{10} \gamma_{10}^2}, \quad \text{(B120)}$$

$$\Delta I_{\text{NaK}}^{\text{Na}_i} = \frac{C_m I_{\text{NaK},0} Q}{\alpha_{10} \beta_{10}^2 \gamma_{10}} n_{H\text{Nai}} (\overline{V}_m + 150)$$

$$\times [\text{K}]_e^{n_{H\text{Ke}}} \text{Na}_{d\text{Nai}}^{n_{H\text{Nai}}} [\overline{\text{Na}}]_i^{n_{H\text{Nai}} - 1}. \quad \text{(B121)}$$

Herein,

$$\alpha_{10} = [\text{K}]_e^{n_{HKe}} + \text{K}_{dKe}^{n_{HKe}}, \tag{B122}$$

$$\beta_{10} = [\overline{\text{Na}}]_i^{n_{HNai}} + \text{Na}_{dNai}^{n_{HNai}}, \tag{B123}$$

$$\gamma_{10} = (\overline{V}_m + 200). \tag{B124}$$

11. Sodium-potassium-chloride cotransport

$$I_{\text{NaKCl}}^{\text{Cl}} = -10^9 z_{\text{Cl}} R_{\text{NaKCl,cGMP}} A_m L_{\text{NaKCl}} RFT$$
$$\times \ln\left(\frac{[\text{Na}]_e}{[\text{Na}]_i} \frac{[\text{K}]_e}{[\text{K}]_i} \frac{[\text{Cl}]_e^2}{[\text{Cl}]_i^2} \right) [\text{pA}]$$
$$\simeq \overline{I}_{\text{NaKCl}}^{\text{Cl}} + \Delta I_{\text{NaKCl}}^{\text{Cl,Na}_i}[\delta_{\text{Na}}]_i + \Delta I_{\text{NaKCl}}^{\text{Cl,K}_i}[\delta_{\text{K}}]_i$$
$$+ \Delta I_{\text{NaKCl}}^{\text{Cl,Cl}_i}[\delta_{\text{Cl}}]_i + \Delta I_{\text{NaKCl}}^{\text{Cl,cGMP}}[\delta_{\text{cGMP}}], \tag{B125}$$

$$I_{\text{NaKCl}}^{\text{Na}} \equiv -\frac{1}{2} I_{\text{NaKCl}}^{\text{Cl}}$$
$$\simeq \overline{I}_{\text{NaKCl}}^{\text{Na}} + \Delta I_{\text{NaKCl}}^{\text{Na,Na}_i}[\delta_{\text{Na}}]_i + \Delta I_{\text{NaKCl}}^{\text{Na,K}_i}[\delta_{\text{K}}]_i$$
$$+ \Delta I_{\text{NaKCl}}^{\text{Na,Cl}_i}[\delta_{\text{Cl}}]_i + \Delta I_{\text{NaKCl}}^{\text{Na,cGMP}}[\delta_{\text{cGMP}}], \tag{B126}$$

$$I_{\text{NaKCl}}^{\text{K}} \equiv -\frac{1}{2} I_{\text{NaKCl}}^{\text{Cl}}$$
$$\simeq \overline{I}_{\text{NaKCl}}^{\text{K}} + \Delta I_{\text{NaKCl}}^{\text{K,Na}_i}[\delta_{\text{Na}}]_i + \Delta I_{\text{NaKCl}}^{\text{K,K}_i}[\delta_{\text{K}}]_i$$
$$+ \Delta I_{\text{NaKCl}}^{\text{K,Cl}_i}[\delta_{\text{Cl}}]_i + \Delta I_{\text{NaKCl}}^{\text{K,cGMP}}[\delta_{\text{cGMP}}], \tag{B127}$$

on quasiequilibrium conditions with relevant variables

$$L_{\text{NaKCl}} = 1.79 \times 10^{-17} \text{ mole}^2/(\text{s J cm}^2),$$

$$R_{\text{NaKCl,cGMP}} = 1 + \frac{3.5[\text{cGMP}]}{[\text{cGMP}] + 6.4 \times 10^{-3} \text{ mM}}, \tag{B128}$$

and the fluctuation terms

$$\Delta I_{\text{NaKCl}}^{\text{Cl,Na}_i} = \frac{\alpha_{11}\beta_{11}}{[\overline{\text{Na}}]_i}, \tag{B129}$$

$$\Delta I_{\text{NaKCl}}^{\text{Cl,K}_i} = \frac{\alpha_{11}\beta_{11}}{[\overline{\text{K}}]_i}, \tag{B130}$$

$$\Delta I_{\text{NaKCl}}^{\text{Cl,Cl}_i} = \frac{2\alpha_{11}\beta_{11}}{[\overline{\text{Cl}}]_i}, \tag{B131}$$

$$\Delta I_{\text{NaKCl}}^{\text{Cl,cGMP}} = \frac{-8750\alpha_{11}\gamma_{11}}{(4 + 625[\overline{\text{cGMP}}])^2}, \tag{B132}$$

$$\Delta I_{\text{NaKCl}}^{\text{Na,Na}_i} = \Delta I_{\text{NaKCl}}^{\text{K,Na}_i} = \frac{-\Delta I_{\text{NaKCl}}^{\text{Cl,Na}_i}}{2}, \tag{B133}$$

$$\Delta I_{\text{NaKCl}}^{\text{Na,K}_i} = \Delta I_{\text{NaKCl}}^{\text{K,K}_i} = \frac{-\Delta I_{\text{NaKCl}}^{\text{Cl,K}_i}}{2}, \tag{B134}$$

$$\Delta I_{\text{NaKCl}}^{\text{Na,Cl}_i} = \Delta I_{\text{NaKCl}}^{\text{K,Cl}_i} = \frac{-\Delta I_{\text{NaKCl}}^{\text{Cl,Cl}_i}}{2}, \tag{B135}$$

$$\Delta I_{\text{NaKCl}}^{\text{Na,cGMP}} = \Delta I_{\text{NaKCl}}^{\text{K,cGMP}} = \frac{-\Delta I_{\text{NaKCl}}^{\text{Cl,cGMP}}}{2}. \tag{B136}$$

Herein,

$$\alpha_{11} = 10^9 z_{\text{Cl}} A_m L_{\text{NaKCl}} RFT, \tag{B137}$$

$$\beta_{11} = 1 + \frac{3.5[\overline{\text{cGMP}}]}{[\overline{\text{cGMP}}] + 6.4 \times 10^{-3}}, \tag{B138}$$

$$\gamma_{11} = \ln\left(\frac{[\text{Na}]_e}{[\overline{\text{Na}}]_i} \frac{[\text{K}]_e}{[\overline{\text{K}}]_i} \frac{[\text{Cl}]_e^2}{[\overline{\text{Cl}}]_i^2} \right). \tag{B139}$$

12. Intercellular ionic communication

$$I_{S,\text{GJ}} = -P z_S^2 \frac{V_{\text{GJ}}F^2}{RT} \frac{[S]_C - [S]_i e^{-z_S V_{\text{GJ}} F/RT}}{1 - e^{-z_S V_{\text{GJ}} F/RT}}$$
$$\simeq \overline{I}_{S,\text{GJ}} + \Delta I_{S,\text{GJ}}^{SC}[\delta_S]_C + \Delta I_{S,\text{GJ}}^{S_i}[\delta_S]_i + \Delta I_{S,\text{GJ}}^{V_{mC}}\delta_{V_{mC}}$$
$$+ \Delta I_{S,\text{GJ}}^{V_m}\delta_{V_m} + \Delta I_{S,\text{GJ}}^{\text{Ca}_i}[\delta_{\text{Ca}}]_i + \Delta I_{S,\text{GJ}}^{\text{Na}_i}[\delta_{\text{Na}}]_i$$
$$+ \Delta I_{S,\text{GJ}}^{K_i}[\delta_K]_i + \Delta I_{S,\text{GJ}}^{\text{Cl}_i}[\delta_{\text{Cl}}]_i \tag{B140}$$

on quasiequilibrium conditions with relevant variables

$$G_{\text{GJ}} = 2 \text{ nS},$$
$$V_{\text{GJ}} = V_{mC} - V_m, \tag{B141}$$

$$P = \frac{G_{\text{GJ}}RT}{F^2 \sum_{S'} \left(z_{S'}^2 [S']_i \right)}, \tag{B142}$$

where S and S' represent all accessible ions: Ca^{2+}, Na$^+$, K$^+$, Cl$^-$. The suffix C denotes the variables of nearby SMCs coupled to the local one. The fluctuation terms are given by

$$\Delta I_{S,\text{GJ}}^{SC} = \frac{-G_{\text{GJ}}\gamma_{12}z_S^2}{\left(1 - \alpha_{12}^{z_S}\right)\beta_{12}}, \tag{B143}$$

$$\Delta I_{S,\text{GJ}}^{S} = \frac{G_{\text{GJ}}\gamma_{12}z_S^2 \alpha_{12}^{z_S}}{\left(1 - \alpha_{12}^{z_S}\right)\beta_{12}}, \tag{B144}$$

$$\Delta I_{S,\text{GJ}}^{V_{mC}} = \frac{G_{\text{GJ}}z_S^3 \alpha_{12}^{z_S}\gamma_{12}F\left([\overline{S}]_C - [\overline{S}]_i\right)}{\left(1 - \alpha_{12}^{z_S}\right)^2 \beta_{12} RT}$$
$$- \frac{G_{\text{GJ}}z_S^2\left([\overline{S}]_C - [\overline{S}]_i \alpha_{12}^{z_S}\right)}{\left(1 - \alpha_{12}^{z_S}\right)\beta_{12}}, \tag{B145}$$

$$\Delta I_{S,\text{GJ}}^{V_m} = -\Delta I_{S,\text{GJ}}^{V_{mC}}, \tag{B146}$$

$$\Delta I_{S,\text{GJ}}^{\text{Ca}_i} = \frac{G_{\text{GJ}}\gamma_{12}z_{\text{Ca}}^2 z_S^2\left([\overline{S}]_C - [\overline{S}]_i \alpha_{12}^{z_S}\right)}{\left(1 - \alpha_{12}^{z_S}\right)\beta_{12}^2}, \tag{B147}$$

$$\Delta I_{S,\text{GJ}}^{\text{Na}_i} = \frac{G_{\text{GJ}}\gamma_{12}z_{\text{Na}}^2 z_S^2\left([\overline{S}]_C - [\overline{S}]_i \alpha_{12}^{z_S}\right)}{\left(1 - \alpha_{12}^{z_S}\right)\beta_{12}^2}, \tag{B148}$$

$$\Delta I_{S,\text{GJ}}^{K_i} = \frac{G_{\text{GJ}}\gamma_{12}z_K^2 z_S^2\left([\overline{S}]_C - [\overline{S}]_i \alpha_{12}^{z_S}\right)}{\left(1 - \alpha_{12}^{z_S}\right)\beta_{12}^2}, \tag{B149}$$

$$\Delta I_{S,\text{GJ}}^{\text{Cl}_i} = \frac{G_{\text{GJ}}\gamma_{12}z_{\text{Cl}}^2 z_S^2\left([\overline{S}]_C - [\overline{S}]_i \alpha_{12}^{z_S}\right)}{\left(1 - \alpha_{12}^{z_S}\right)\beta_{12}^2}. \tag{B150}$$

Herein,

$$\alpha_{12} = \exp\left[\frac{-F(\overline{V}_{mC} - \overline{V}_m)}{RT}\right], \qquad (B151)$$

$$\beta_{12} = z_{\text{Ca}}^2[\overline{\text{Ca}}]_i + z_{\text{Na}}^2[\overline{\text{Na}}]_i + z_{\text{K}}^2[\overline{\text{K}}]_i + z_{\text{Cl}}^2[\overline{\text{Cl}}]_i, \quad (B152)$$

$$\gamma_{12} = \overline{V}_{mC} - \overline{V}_m. \qquad (B153)$$

APPENDIX C: MATHEMATICAL MODEL EQUATIONS FOR SARCOPLASMIC RETICULUM

1. Calcium-induced calcium-release mechanism of sarcoplasmic reticulum

$$I_{\text{SERCA}} = I_{\text{SERCA},0}\frac{[\text{Ca}]_i}{[\text{Ca}]_i + K_{m,up}}$$
$$\simeq \overline{I}_{\text{SERCA}} + \Delta I_{\text{SERCA}}^{\text{Ca}_i}[\delta_{\text{Ca}}]_i, \qquad (C1)$$

$$I_{\text{tr}} = ([\text{Ca}]_u - [\text{Ca}]_r)\frac{z_{\text{Ca}}\text{vol}_u F}{\tau_{\text{tr}}}$$
$$\simeq \overline{I}_{\text{tr}} + \Delta I_{\text{tr}}^{\text{Ca}_u}[\delta_{\text{Ca}}]_u + \Delta I_{\text{tr}}^{\text{Ca}_r}[\delta_{\text{Ca}}]_r, \qquad (C2)$$

$$I_{\text{rel}} = ([\text{Ca}]_r - [\text{Ca}]_i)\frac{(R_{10}^2 + R_{\text{leak}})z_{\text{Ca}}\text{vol}_r F}{\tau_{\text{rel}}}$$
$$\simeq \overline{I}_{\text{rel}} + \Delta I_{\text{rel}}^{\text{Ca}_i}[\delta_{\text{Ca}}]_i + \Delta I_{\text{rel}}^{\text{Ca}_r}[\delta_{\text{Ca}}]_r + \Delta I_{\text{rel}}^{R_{10}}\delta_{R_{10}}, \quad (C3)$$

on quasiequilibrium conditions with relevant variables

$$I_{\text{SERCA},0} = 6.68 \text{ pA}, \qquad K_{m,up} = 10^{-3} \text{ mM},$$
$$\tau_{\text{tr}} = 1000.0 \text{ ms}, \qquad \tau_{\text{rel}} = 0.0333 \text{ ms},$$
$$R_{\text{leak}} = 1.07 \times 10^{-5},$$

and the fluctuation terms

$$\Delta I_{\text{SERCA}}^{\text{Ca}_i} = \frac{I_{\text{SERCA},0}K_{m,up}}{([\overline{\text{Ca}}]_i + K_{m,up})^2}, \qquad (C4)$$

$$\Delta I_{\text{tr}}^{\text{Ca}_r} = \frac{-z_{\text{Ca}}\text{vol}_u F}{\tau_{\text{tr}}}, \qquad (C5)$$

$$\Delta I_{\text{tr}}^{\text{Ca}_u} = \frac{z_{\text{Ca}}\text{vol}_u F}{\tau_{\text{tr}}}, \qquad (C6)$$

$$\Delta I_{\text{rel}}^{\text{Ca}_r} = \frac{z_{\text{Ca}}\text{vol}_r F}{\tau_{\text{rel}}}\left(\overline{R}_{10}^2 + R_{\text{leak}}\right), \qquad (C7)$$

$$\Delta I_{\text{rel}}^{\text{Ca}_i} = \frac{-z_{\text{Ca}}\text{vol}_r F}{\tau_{\text{rel}}}\left(\overline{R}_{10}^2 + R_{\text{leak}}\right), \qquad (C8)$$

$$\Delta I_{\text{rel}}^{R_{10}} = \frac{2z_{\text{Ca}}\text{vol}_r F\overline{R}_{10}}{\tau_{\text{rel}}}([\overline{\text{Ca}}]_r - [\overline{\text{Ca}}]_i). \qquad (C9)$$

2. Ryanodine receptor

$$\frac{dR_{10}}{dt} = K_{r1}[\text{Ca}]_i^2 R_{00} - (K_{-r1} + K_{r2}[\text{Ca}]_i)R_{10} + K_{-r2}R_{11}, \qquad (C10)$$

$$\frac{dR_{11}}{dt} = K_{r2}[\text{Ca}]_i R_{10} - (K_{-r1} + K_{-r2})R_{11} + K_{r1}[\text{Ca}]_i^2 R_{01}, \qquad (C11)$$

$$\frac{dR_{01}}{dt} = K_{r2}[\text{Ca}]_i R_{00} - \left(K_{-r2} + K_{r1}[\text{Ca}]_i^2\right)R_{01} + K_{-r1}R_{11}, \qquad (C12)$$

$$R_{00} = 1 - R_{01} - R_{10} - R_{11}. \qquad (C13)$$

On the quasiequilibrium conditions, the equations can be rearranged by defining $R_{ij} = \overline{R}_{ij} + \delta_{R_{ij}}$ as the time-independent constant term ($d\overline{R}_{ij}/dt = 0$) plus the time-dependent fluctuation $\delta_{R_{ij}}$:

$$\frac{d\delta_{R_{10}}}{dt} \simeq \Delta_{R_{10}}^{\text{Ca}_i}[\delta_{\text{Ca}}]_i + \Delta_{R_{10}}^{R_{10}}\delta_{R_{10}} + \Delta_{R_{10}}^{R_{11}}\delta_{R_{11}} + \Delta_{R_{10}}^{R_{01}}\delta_{R_{01}}, \quad (C14)$$

$$\frac{d\delta_{R_{11}}}{dt} \simeq \Delta_{R_{11}}^{\text{Ca}_i}[\delta_{\text{Ca}}]_i + \Delta_{R_{11}}^{R_{10}}\delta_{R_{10}} + \Delta_{R_{11}}^{R_{11}}\delta_{R_{11}} + \Delta_{R_{11}}^{R_{01}}\delta_{R_{01}}, \quad (C15)$$

$$\frac{d\delta_{R_{01}}}{dt} \simeq \Delta_{R_{01}}^{\text{Ca}_i}[\delta_{\text{Ca}}]_i + \Delta_{R_{01}}^{R_{10}}\delta_{R_{10}} + \Delta_{R_{01}}^{R_{11}}\delta_{R_{11}} + \Delta_{R_{01}}^{R_{01}}\delta_{R_{01}}, \quad (C16)$$

with relevant variables

$$K_{r1} = 2500.0 \text{ mM}^{-2} \text{ ms}^{-1},$$
$$K_{r2} = 1.05 \text{ mM}^{-1} \text{ ms}^{-1},$$
$$K_{-r1} = 0.0076 \text{ ms}^{-1}, \quad K_{-r2} = 0.084 \text{ ms}^{-1},$$

and the fluctuation terms

$$\Delta_{R_{10}}^{R_{10}} = -K_{-r1} - [\overline{\text{Ca}}]_i^2 K_{r1} - [\overline{\text{Ca}}]_i K_{r2}, \qquad (C17)$$

$$\Delta_{R_{10}}^{R_{11}} = K_{-r2} - [\overline{\text{Ca}}]_i^2 K_{r1}, \qquad (C18)$$

$$\Delta_{R_{10}}^{R_{01}} = -[\overline{\text{Ca}}]_i^2 K_{r1}, \qquad (C19)$$

$$\Delta_{R_{10}}^{\text{Ca}_i} = 2[\overline{\text{Ca}}]_i K_{r1} - 2[\overline{\text{Ca}}]_i K_{r1}\overline{R}_{01} - K_{r2}\overline{R}_{10}$$
$$- 2[\overline{\text{Ca}}]_i K_{r1}\overline{R}_{10} - 2[\overline{\text{Ca}}]_i K_{r1}\overline{R}_{11}, \qquad (C20)$$

$$\Delta_{R_{11}}^{R_{10}} = [\overline{\text{Ca}}]_i K_{r2}, \quad \Delta_{R_{11}}^{R_{01}} = [\overline{\text{Ca}}]_i^2 K_{r1}, \qquad (C21)$$

$$\Delta_{R_{11}}^{R_{11}} = -K_{-r1} - K_{-r2}, \qquad (C22)$$

$$\Delta_{R_{11}}^{\text{Ca}_i} = 2[\overline{\text{Ca}}]_i K_{r1}\overline{R}_{01} + K_{r2}\overline{R}_{10}, \qquad (C23)$$

$$\Delta_{R_{01}}^{R_{10}} = -[\overline{\text{Ca}}]_i K_{r2}, \qquad (C24)$$

$$\Delta_{R_{01}}^{R_{11}} = K_{-r1} - [\overline{\text{Ca}}]_i K_{r2}, \qquad (C25)$$

$$\Delta_{R_{01}}^{R_{01}} = -K_{-r2} - [\overline{\text{Ca}}]_i^2 K_{r1} - [\overline{\text{Ca}}]_i K_{r2}, \qquad (C26)$$

$$\Delta_{R_{01}}^{\text{Ca}_i} = -2[\overline{\text{Ca}}]_i K_{r1}\overline{R}_{01} - K_{r2}\overline{R}_{01} - K_{r2}\overline{R}_{10}$$
$$- K_{r2}\overline{R}_{11} + K_{r2}. \qquad (C27)$$

3. IP₃ receptor

$$I_{\text{IP3}} = I_{\text{IP3},0}z_{\text{Ca}}\text{vol}_{\text{Ca}}F([\text{Ca}]_u - [\text{Ca}]_i)$$
$$\times \left(\frac{[\text{IP}_3]}{[\text{IP}_3] + K_{\text{IP3}}}\frac{[\text{Ca}]_i h_{\text{IP3}}}{[\text{Ca}]_i + K_{\text{act,IP3}}}\right)^3$$
$$\simeq \overline{I}_{\text{IP3}} + \Delta I_{\text{IP3}}^{\text{Ca}_i}[\delta_{\text{Ca}}]_i + \Delta I_{\text{IP3}}^{\text{Ca}_u}[\delta_{\text{Ca}}]_u$$
$$+ \Delta I_{\text{IP3}}^{\text{IP3}}[\delta_{\text{IP3}}] + \Delta I_{\text{IP3}}^{h_{\text{IP3}}}\delta_{h_{\text{IP3}}}, \qquad (C28)$$

$$\frac{dh_{IP3}}{dt} = K_{on,IP3}[K_{inh,IP3} - ([Ca]_i + K_{inh,IP3})h_{IP3}]$$

$$\simeq \frac{d\delta_{h_{IP3}}}{dt} = \Delta^{Ca_i}_{h_{IP3}}[\delta_{Ca}]_i + \Delta I^{h_{IP3}}_{h_{IP3}}\delta_{h_{IP3}}, \quad \text{(C29)}$$

on quasiequilibrium conditions with relevant variables

$$I_{IP3,0} = 0.00288 \text{ ms}^{-1}, \quad K_{IP3} = 1.2 \times 10^{-4} \text{ mM},$$

$$K_{act,IP3} = 1.7 \times 10^{-4} \text{ mM}, \quad K_{inh,IP3} = 10^{-4} \text{ mM},$$

$$K_{on,IP3} = 1.4 \text{ ms}^{-1} \text{ mM}^{-1},$$

and the fluctuation terms

$$\Delta I^{h_{IP3}}_{IP3} = \frac{3\alpha_{14}\overline{h}^2_{IP3}[\overline{Ca}]^3_i[\overline{IP_3}]^3}{\beta^3_{14}\gamma^3_{14}}([\overline{Ca}]_u - [\overline{Ca}]_i), \quad \text{(C30)}$$

$$\Delta I^{Ca_u}_{IP3} = \frac{\alpha_{14}\overline{h}^3_{IP3}[\overline{Ca}]^3_i[\overline{IP_3}]^3}{\beta^3_{14}\gamma^3_{14}}, \quad \text{(C31)}$$

$$\Delta I^{IP3}_{IP3} = \frac{3\alpha_{14}\overline{h}^3_{IP3}[\overline{Ca}]^3_i[\overline{IP_3}]^2 K_{IP3}}{\beta^4_{14}\gamma^3_{14}}([\overline{Ca}]_u - [\overline{Ca}]_i), \quad \text{(C32)}$$

$$\Delta I^{Ca_i}_{IP3} = \frac{\alpha_{14}\overline{h}^3_{IP3}[\overline{IP_3}]^3}{\beta^3_{14}\gamma^4_{14}}\Big\{-4[\overline{Ca}]^3_i K_{act,IP3}$$
$$- [\overline{Ca}]^4_i + 3[\overline{Ca}]^2_i[\overline{Ca}]_u K_{act,IP3}\Big\}, \quad \text{(C33)}$$

$$\Delta^{Ca_i}_{h_{IP3}} = -\overline{h}_{IP3}K_{on,IP3}, \quad \text{(C34)}$$

$$\Delta I^{h_{IP3}}_{h_{IP3}} = -K_{on,IP3}(K_{inh,IP3} + [\overline{Ca}]_i). \quad \text{(C35)}$$

Herein,

$$\alpha_{14} = I_{IP3,0} \times z_{Ca} \times \text{vol}_{Ca} \times F, \quad \text{(C36)}$$

$$\beta_{14} = [\overline{IP_3}] + K_{IP3}, \quad \text{(C37)}$$

$$\gamma_{14} = [\overline{Ca}]_i + K_{act,IP3}. \quad \text{(C38)}$$

APPENDIX D: α₁-ADRENOCEPTOR ACTIVATION AND IP₃ FORMATION

$$\frac{d[G]}{dt} = k_{a,G}(\delta_G + \rho_{r,G})([G_{T,G}] - [G]) - k_{d,G}[G]$$

$$\simeq \frac{d[\delta_G]}{dt} = \Delta^{R^S_G}_G[\delta_{R^S_G}] + \Delta^G_G[\delta_G], \quad \text{(D1)}$$

$$\frac{d[IP_3]}{dt} = \frac{r_{h,G}}{\gamma_G}[PIP_2] - k_{deg,G}[IP_3]$$

$$+ P_{IP3} \sum_C ([IP_3]_C - [IP_3])$$

$$\simeq \frac{d[\delta_{IP3}]}{dt} = \Delta^{Ca_i}_{IP3}[\delta_{Ca}]_i + \Delta^G_{IP3}[\delta_G]$$

$$+ \Delta^{PIP_2}_{IP3}[\delta_{PIP_2}] + \Delta^{IP3}_{IP3}[\delta_{IP3}]$$

$$+ \sum_C \Delta^{IP3C}_{IP3}[\delta_{IP3}]_C, \quad \text{(D2)}$$

$$\frac{d[R^S_{P,G}]}{dt} = \frac{[NE]k_{p,G}[R^S_G]}{K_{1,G} + [NE]} - \frac{[NE]k_{e,G}[R^S_{P,G}]}{K_{2,G} + [NE]}$$

$$\simeq \frac{d[\delta_{R^S_{P,G}}]}{dt} = \Delta^{R^S_G}_{R^S_{P,G}}[\delta_{R^S_G}] + \Delta^{R^S_{P,G}}_{R^S_{P,G}}[\delta_{R^S_{P,G}}], \quad \text{(D3)}$$

$$\frac{d[R^S_G]}{dt} = k_{r,G}\xi_G[R_{T,G}] - k_{r,G}[R^S_{P,G}]$$

$$- \left(k_{r,G} + \frac{k_{p,G}[NE]}{K_{1,G} + [NE]}\right)[R^S_G]$$

$$\simeq \frac{d[\delta_{R^S_G}]}{dt} = \Delta^{R^S_G}_{R^S_G}[\delta_{R^S_G}] + \Delta^{R^S_{P,G}}_{R^S_G}[\delta_{R^S_{P,G}}], \quad \text{(D4)}$$

$$\frac{d[PIP_2]}{dt} = -(r_{h,G} + r_{r,G})[PIP_2] - r_{r,G}\gamma_G[IP_3] + r_{r,G}[PIP_{2,T}]$$

$$\simeq \frac{d[\delta_{PIP_2}]}{dt} = \Delta^{Ca_i}_{PIP_2}[\delta_{Ca}]_i + \Delta^G_{PIP_2}[\delta_G]$$

$$+ \Delta^{PIP_2}_{PIP_2}[\delta_{PIP_2}] + \Delta^{IP3}_{PIP_2}[\delta_{IP3}], \quad \text{(D5)}$$

on quasiequilibrium conditions with relevant variables

$$[R_{T,G}] = 2 \times 10^4, \quad K_{1,G} = 10^{-2} \text{ mM},$$

$$K_{2,G} = 0.2 \text{ mM}, \quad k_{r,G} = 1.75 \times 10^{-7} \text{ ms}^{-1},$$

$$k_{e,G} = 6 \times 10^{-6} \text{ ms}^{-1}, \quad k_{a,G} = 0.17 \times 10^{-3} \text{ ms}^{-1},$$

$$k_{deg,G} = 1.25 \times 10^{-3} \text{ ms}^{-1}, \quad \xi_G = 0.85,$$

$$k_{d,G} = 1.5 \times 10^{-3} \text{ ms}^{-1}, \quad [PIP_{2,T}] = 5 \times 10^7,$$

$$r_{r,G} = 1.5 \times 10^{-5} \text{ ms}^{-1}, \quad K_{c,G} = 4 \times 10^{-4} \text{ mM},$$

$$\alpha_G = 2.781 \times 10^{-8} \text{ ms}^{-1},$$

$$[G_{T,G}] = 10^5, \quad k_{p,G} = 10^{-4} \text{ ms}^{-1},$$

$$P_{IP3} = 0.53 \times 10^{-3} \text{ ms}^{-1},$$

$$\gamma_G = 10^{-15} N_{Av} \times \text{vol}_i,$$

$$\delta_G = \frac{k_{d,G}[G]}{k_{a,G}([G_{T,G}] - [G])}, \quad \text{fixed at initial},$$

$$\rho_{r,G} = \frac{[NE][R^S_G]}{\xi_G[R_{T,G}](K_{1,G} + [NE])}, \quad \text{(D6)}$$

$$r_{h,G} = \alpha_G \frac{[Ca]_i}{[Ca]_i + K_{c,G}}[G], \quad \text{(D7)}$$

and the fluctuation terms

$$\Delta^{R^S_G}_G = \frac{([G_{T,G}] - [\overline{G}])k_{a,G}[NE]}{(K_{1,G} + [NE])R_{T,G}\xi_G}, \quad \text{(D8)}$$

$$\Delta^G_G = -k_{d,G} - \frac{k_{a,G}[NE][\overline{R}^S_G]}{(K_{1,G} + [NE])[R_{T,G}]\xi_G} - k_{a,G}\delta_G, \quad \text{(D9)}$$

$$\Delta^{Ca_i}_{IP3} = \frac{K_{c,G}[\overline{G}][\overline{PIP}_2]\alpha_G}{([\overline{Ca}]_i + K_{c,G})^2\gamma_G}, \quad \text{(D10)}$$

$$\Delta_{\text{IP3}}^{G} = \frac{[\overline{\text{Ca}}]_i[\overline{\text{PIP}_2}]\alpha_G}{([\overline{\text{Ca}}]_i + K_{c,G})\gamma_G}, \tag{D11}$$

$$\Delta_{\text{IP3}}^{\text{PIP}_2} = \frac{[\overline{\text{Ca}}]_i[\overline{G}]\alpha_G}{([\overline{\text{Ca}}]_i + K_{c,G})\gamma_G}, \tag{D12}$$

$$\Delta_{\text{IP3}}^{\text{IP3}} = -k_{\deg,G} - \sum_C P_{\text{IP3}}, \tag{D13}$$

$$\Delta_{\text{IP3}}^{\text{IP3C}} = P_{\text{IP3}}, \tag{D14}$$

$$\Delta_{R_{P,G}^S}^{R_G^S} = \frac{k_{p,G}[\text{NE}]}{K_{1,G} + [\text{NE}]}, \tag{D15}$$

$$\Delta_{R_{P,G}^S}^{R_{P,G}^S} = \frac{-k_{e,G}[\text{NE}]}{K_{2,G} + [\text{NE}]}, \tag{D16}$$

$$\Delta_{R_G^S}^{R_G^S} = -k_{r,G} - \frac{k_{p,G}[\text{NE}]}{K_{1,G} + [\text{NE}]}, \tag{D17}$$

$$\Delta_{R_G^S}^{R_{P,G}^S} = -k_{r,G}, \quad \Delta_{\text{PIP}_2}^{\text{IP3}} = -r_{r,G}\gamma_G, \tag{D18}$$

$$\Delta_{\text{PIP}_2}^{\text{Ca}_i} = -\frac{K_{c,G}[\overline{G}][\overline{\text{PIP}_2}]\alpha_G}{([\overline{\text{Ca}}]_i + K_{c,G})^2}, \tag{D19}$$

$$\Delta_{\text{PIP}_2}^{G} = -\frac{[\overline{\text{Ca}}]_i[\overline{\text{PIP}_2}]\alpha_G}{[\overline{\text{Ca}}]_i + K_{c,G}}, \tag{D20}$$

$$\Delta_{\text{PIP}_2}^{\text{PIP}_2} = -r_{r,G} - \frac{[\overline{\text{Ca}}]_i[\overline{G}]\alpha_G}{[\overline{\text{Ca}}]_i + K_{c,G}}. \tag{D21}$$

Herein, the IP$_3$ flux through gap junctions is also included, and [IP$_3$]$_C$ denotes the concentrations for nearby SMCs coupled to the local one.

APPENDIX E: sGC ACTIVATION AND cGMP FORMATION

$$\frac{dV_{\text{cGMP}}}{dt} = \frac{V_{\text{cGMP},0} - V_{\text{cGMP}}}{\tau_{\text{sGC}}}$$

$$\simeq \frac{d\delta_{V_{\text{cGMP}}}}{dt} = \Delta_{V_{\text{cGMP}}}^{V_{\text{cGMP}}}\delta_{V_{\text{cGMP}}}, \tag{E1}$$

$$\frac{d[\text{cGMP}]}{dt} = V_{\text{cGMP}} - k_{pde,\text{cGMP}}\frac{[\text{cGMP}]^2}{[\text{cGMP}] + K_{m,pde}}$$

$$\simeq \frac{d\delta_{\text{cGMP}}}{dt}$$

$$= \Delta_{\text{cGMP}}^{V_{\text{cGMP}}}\delta_{V_{\text{cGMP}}} + \Delta_{\text{cGMP}}^{\text{cGMP}}\delta_{\text{cGMP}}, \tag{E2}$$

on quasiequilibrium conditions with relevant variables

$$k_{1,\text{sGC}} = 2 \times 10^3 \text{ mM}^{-1} \text{ ms}^{-1},$$
$$k_{-1,\text{sGC}} = 15 \times 10^{-3} \text{ ms}^{-1},$$
$$k_{2,\text{sGC}} = 0.64 \times 10^{-5} \text{ ms}^{-1},$$
$$k_{-2,\text{sGC}} = 0.1 \times 10^{-6} \text{ ms}^{-1},$$
$$k_{3,\text{sGC}} = 4.2 \text{ mM}^{-1} \text{ ms}^{-1},$$
$$k_{D,\text{sGC}} = 0.4 \times 10^{-3} \text{ ms}^{-1},$$

$$k_{D\tau,\text{sGC}} = 10^{-4} \text{ ms}^{-1}, \quad B5_{\text{sGC}} = k_{2,\text{sGC}}/k_{3,\text{sGC}},$$
$$k_{pde,\text{cGMP}} = 6.95 \times 10^{-5} \text{ ms}^{-1}, \quad k_{m,pde} = 10^{-3} \text{ mM},$$
$$V_{\text{cGMP,max}} = 1.26 \times 10^{-7} \text{ mM/ms},$$

$$V_{\text{cGMP},0} = V_{\text{cGMP,max}}\frac{B5_{\text{sGC}}[\text{NO}] + [\text{NO}]^2}{A0_{\text{sGC}} + A1_{\text{sGC}}[\text{NO}] + [\text{NO}]^2}, \tag{E3}$$

$$A0_{\text{sGC}} = \frac{(k_{-1,\text{sGC}} + k_{2,\text{sGC}})k_{D,\text{sGC}}}{k_{1,\text{sGC}}k_{3,\text{sGC}}} + \frac{k_{-1,\text{sGC}}k_{-2,\text{sGC}}}{k_{1,\text{sGC}}k_{3,\text{sGC}}}, \tag{E4}$$

$$A1_{\text{sGC}} = \frac{(k_{1,\text{sGC}} + k_{3,\text{sGC}})k_{D,\text{sGC}}}{k_{1,\text{sGC}}k_{3,\text{sGC}}}$$

$$+ \frac{(k_{2,\text{sGC}} + k_{-2,\text{sGC}})k_{1,\text{sGC}}}{k_{1,\text{sGC}}k_{3,\text{sGC}}}, \tag{E5}$$

$$\tau_{\text{msGC}} = \frac{1}{k_{3,\text{sGC}}[\text{NO}] + k_{D\tau,\text{sGC}}}, \tag{E6}$$

$$\tau_{\text{ssGC}} = \frac{1}{k_{-2,\text{sGC}} + k_{D\tau,\text{sGC}}} - \tau_{\text{msGC}}, \tag{E7}$$

$$\tau_{\text{sGC}} = \tau_{\text{msGC}} + \frac{\tau_{\text{ssGC}}}{1 + e^{-10\frac{V_{\text{cGMP}} - V_{\text{cGMP},0}}{V_{\text{cGMP,max}}}}}, \tag{E8}$$

and the fluctuation terms

$$\Delta_{V_{\text{cGMP}}}^{V_{\text{cGMP}}} = \frac{10\alpha_{16}(\overline{V}_{\text{cGMP}} - V_{\text{cGMP},0})\tau_{\text{ssGC}}}{V_{\text{cGMP,max}}[\tau_{\text{ssGC}} + (1 + \alpha_{16})\tau_{\text{msGC}}]^2}$$

$$- \frac{1}{\tau_{\text{msGC}} + \frac{\tau_{\text{ssGC}}}{1+\alpha_{16}}}, \tag{E9}$$

$$\Delta_{\text{cGMP}}^{V_{\text{cGMP}}} = 1, \tag{E10}$$

$$\Delta_{\text{cGMP}}^{\text{cGMP}} = -\frac{k_{pde,\text{cGMP}}[\overline{\text{cGMP}}]}{([\overline{\text{cGMP}}] + K_{m,pde})^2}([\overline{\text{cGMP}}] + 2K_{m,pde}). \tag{E11}$$

Herein

$$\alpha_{16} = \exp\left(-10\frac{\overline{V}_{\text{cGMP}} - V_{\text{cGMP},0}}{V_{\text{cGMP,max}}}\right). \tag{E12}$$

APPENDIX F: IONIC BALANCES AND MEMBRANE POTENTIAL

$$\frac{d[\text{Ca}]_u}{dt} = \frac{I_{\text{SERCA}} - I_{\text{tr}} - I_{\text{IP3}}}{z_{\text{Ca}}\text{vol}_u F} \tag{F1}$$

$$\simeq \frac{d[\delta_{\text{Ca}}]_u}{dt} = \frac{\sum_{v_i}\Delta I_{\text{SERCA}}^{v_i} - \Delta I_{\text{tr}}^{v_i} - \Delta I_{\text{IP3}}^{v_i}}{z_{\text{Ca}}\text{vol}_u F}, \tag{F2}$$

$$\frac{d[\text{Ca}]_r}{dt} = \frac{I_{\text{tr}} - I_{\text{rel}}}{z_{\text{Ca}}\text{vol}_r F}\left[1 + \frac{[\overline{\text{CSQN}}]K_{\text{CSQN}}}{(K_{\text{CSQN}} + [\text{Ca}]_r)^2}\right]^{-1} \simeq \frac{d[\delta_{\text{Ca}}]_r}{dt}$$

$$= \frac{\sum_{v_i}\Delta I_{\text{tr}}^{v_i} - \Delta I_{\text{rel}}^{v_i}}{z_{\text{Ca}}\text{vol}_r F}\left[1 + \frac{[\overline{\text{CSQN}}]K_{\text{CSQN}}}{(K_{\text{CSQN}} + [\overline{\text{Ca}}]_r)^2}\right]^{-1}, \tag{F3}$$

$$\frac{d[\text{Ca}]_i}{dt} = -\frac{I_{\text{Ca,tot}}}{z_{\text{Ca}}\text{vol}_{\text{Ca}}F}\left[1 + \frac{[\overline{S}_{\text{CM}}]K_d}{(K_d + [\text{Ca}]_i)^2} + \frac{[\overline{B}_F]K_{dB}}{(K_{dB} + [\text{Ca}]_i)^2}\right]^{-1} \simeq \frac{d[\delta_{\text{Ca}}]_i}{dt}$$

$$= -\frac{\Delta I_{\text{Ca,tot}}}{z_{\text{Ca}}\text{vol}_{\text{Ca}}F}\left[1 + \frac{[\overline{S}_{\text{CM}}]K_d}{(K_d + [\overline{\text{Ca}}]_i)^2} + \frac{[\overline{B}_F]K_{dB}}{(K_{dB} + [\overline{\text{Ca}}]_i)^2}\right]^{-1}, \tag{F4}$$

$$\frac{d[\text{Na}]_i}{dt} = -\frac{I_{\text{Na,tot}}}{z_{\text{Na}}\text{vol}_i F} \simeq \frac{d[\delta_{\text{Na}}]_i}{dt} = -\frac{\Delta I_{\text{Na,tot}}}{z_{\text{Na}}\text{vol}_i F}, \tag{F5}$$

$$\frac{d[\text{K}]_i}{dt} = -\frac{I_{\text{K,tot}}}{z_{\text{K}}\text{vol}_i F} \simeq \frac{d[\delta_{\text{K}}]_i}{dt} = -\frac{\Delta I_{\text{K,tot}}}{z_{\text{K}}\text{vol}_i F}, \tag{F6}$$

$$\frac{d[\text{Cl}]_i}{dt} = -\frac{I_{\text{Cl,tot}}}{z_{\text{Cl}}\text{vol}_i F} \simeq \frac{d[\delta_{\text{Cl}}]_i}{dt} = -\frac{\Delta I_{\text{Cl,tot}}}{z_{\text{Cl}}\text{vol}_i F}, \tag{F7}$$

$$\frac{dV_m}{dt} = \frac{-I_{V,\text{tot}} + I_{\text{stim}}}{C_m} \simeq \frac{d\delta_{V_m}}{dt} = \frac{\sum_{v_i}(-I_{V,\text{tot}}) + I_{\text{stim}}}{C_m}, \tag{F8}$$

for quasiequilibrium conditions with v_i being the model component. Relevant variables are

$$[\overline{\text{CSQN}}] = 15.0 \text{ mM}, \quad K_{\text{CSQN}} = 0.8 \text{ mM},$$

$$[\overline{S}_{\text{CM}}] = 0.1 \text{ mM}, \quad K_d = 0.00026 \text{ mM},$$

$$[\overline{B}_F] = 0.1 \text{ mM}, \quad K_{dB} = 0.0005298 \text{ mM},$$

$$\Delta I_{\text{Ca,tot}} = \sum_{v_i,C} \Delta I_{\text{SOCCa}}^{v_i} + \Delta I_{\text{VOCC}}^{v_i} - 2\Delta I_{\text{NCX}}^{v_i} + \Delta I_{\text{PMCA}}^{v_i} + \Delta I_{\text{CaNSC}}^{v_i} + \Delta I_{\text{SERCA}}^{v_i} - \Delta I_{\text{rel}}^{v_i} - \Delta I_{\text{IP3}}^{v_i} + \Delta I_{\text{Ca,GJ}}^{v_i,C}, \tag{F9}$$

$$\Delta I_{\text{Na,tot}} = \sum_{v_i,C} \Delta I_{\text{NaKCl}}^{\text{Na},v_i} + \Delta I_{\text{SOCNa}}^{v_i} + 3\Delta I_{\text{NaK}}^{v_i} + 3\Delta I_{\text{NCX}}^{v_i} + \Delta I_{\text{NaNSC}}^{v_i} + \Delta I_{\text{Na,GJ}}^{v_i,C}, \tag{F10}$$

$$\Delta I_{\text{K,tot}} = \sum_{v_i,C} \Delta I_{\text{NaKCl}}^{\text{K},v_i} + \Delta I_{\text{K}v}^{v_i} + \Delta I_{\text{BKCa}}^{v_i} + \Delta I_{\text{KNSC}}^{v_i} + \Delta I_{\text{Kleak}}^{v_i} - 2\Delta I_{\text{NaK}}^{v_i} + \Delta I_{\text{K,GJ}}^{v_i,C}, \tag{F11}$$

$$\Delta I_{\text{Cl,tot}} = \sum_{v_i,C} \Delta I_{\text{NaKCl}}^{\text{Cl},v_i} + \Delta I_{\text{ClCa}}^{v_i} + \Delta I_{Cl.\text{GJ}}^{v_i,C}, \tag{F12}$$

$$I_{V,\text{tot}} = \sum_{v_i,C} \Delta I_{\text{VOCC}}^{v_i} + \Delta I_{\text{K}v}^{v_i} + \Delta I_{\text{BKCa}}^{v_i} + \Delta I_{\text{Kleak}}^{v_i} + \Delta I_{\text{NSC}}^{v_i} + \Delta I_{\text{SOC}}^{v_i} + \Delta I_{\text{ClCa}}^{v_i} + \Delta I_{\text{PMCA}}^{v_i} + \Delta I_{\text{NaK}}^{v_i}$$

$$+ \Delta I_{\text{NCX}}^{v_i} + \Delta I_{\text{Ca,GJ}}^{v_i,C} + \Delta I_{\text{Na,GJ}}^{v_i,C} + \Delta I_{\text{K,GJ}}^{v_i,C} + \Delta I_{\text{Cl.GJ}}^{v_i,C}. \tag{F13}$$

Herein, ΔI^C denotes the variation of current transferring from nearby cells to the local one.

---

[1] T. B. Bolton, T. Tomita, and G. Vassort, in *Smooth Muscle: An Assessment of Current Knowledge*, edited by E. Bulbring, A. F. Brading, A. W. Jones, and T. Tomita (University of Texas Press, Austin, 1981), Chap. 3.

[2] D. F. Van Helden, J. Physiol. **471**, 465 (1993).

[3] H. Hashitani, D. F. Van Helden, and H. Suzuki, Br. J. Pharmacol. **118**, 1627V1632 (1996).

[4] K. Shimamura, F. Sekiguchi, and S. Sunano, Clin. Exp. Pharmacol. Physiol. **26**, 275 (1999).

[5] H. Nilsson and C. Aalkjaer, Mol. Interv. **3**, 79V89 (2003).

[6] R. E. Haddock and C. E. Hill, J. Physiol. **566.3**, 645 (2005).

[7] C. Aalkjaer and H. Nilsson, Br. J. Pharmacol. **144**, 605V616 (2005).

[8] K. Kawasaki, K. Seki, and S. Hosoda, Experientia **37**, 1291 (1981).

[9] N. I. Gokina, R. D. Bevan, C. L. Walters, and J. A. Bevan, Circ. Res. **78**, 148 (1996).

[10] M. Omote, N. Kajimoto, and H. Mizusawa, Acta Physiol. Scand. **147**, 9 (1993).

[11] Y. Masuda, K. Okui, and Y. Fukuda, Jpn. J. Physiol. **32**, 453 (1982).

[12] K. A. Dora, J. Xia, and B. R. Duling, Am. J. Physiol.: Heart Circ. Physiol. **285**, H119 (2003).

[13] M. Lamboley, A. Schuster, J. Beny, and J. Meister, Am. J. Physiol.: Heart Circ. Physiol. **285**, H562 (2003).

[14] D. Seppey, R. Sauser, M. Koenigsberger, J. Beny, and J. Meister, Am. J. Physiol.: Heart Circ. Physiol. **298**, H488 (2010).

[15] L. Shaw, S. O'Neill, C. J. Jones, C. Austin, and M. J. Taggart, Br. J. Pharmacol. **141**, 678 (2004).

[16] B. R. Duling and R. M. Berne, Circ. Res. **26**, 163 (1970).

[17] A. G. Tsai and M. Intaglietta, Int. J. Microcirc.: Clin. Exp. **12**, 75V88 (1993).

[18] M. Rucker, O. Strobel, B. Vollmar, F. Roesken, and M. D. Menger, Am. J. Physiol.: Heart Circ. Physiol. **279**, H550 (2000).

[19] T. Sakurai and N. Terui, Am. J. Physiol.: Heart Circ. Physiol. **291**, H1761 (2006).

[20] W. Funk, B. Endrich, K. Messmer, and M. Intaglietta, Int. J. Microcirc.: Clin. Exp. **2**, 11 (1983).

[21] C. Meyer, G. De Vries, S. T. Davidge, and D. C. Mayes, J. Appl. Physiol. **92**, 888 (2002).

[22] A. Kapela, A. Bezerianos, and N. M. Tsoukias, J. Theor. Biol. **253**, 238 (2008).

[23] A. Kapela, S. Nagaraja, and N. M. Tsoukias, Am. J. Physiol.: Heart Circ. Physiol. **298**, H52 (2010).

[24] D. Parthimos, R. E. Haddock, C. E. Hill, and T. M. Griffith, Biophys. J. **93**, 1534 (2007).

[25] M. Koenigsberger, R. Sauser, D. Seppey, J. L. Beny, and J. J. Meister, Biophys. J. **95**, 2728 (2008).

[26] A. Goldbeter, G. Dupont, and M. J. Berridge, Proc. Natl. Acad. Sci. USA **87**, 1461 (1990).

[27] J. M. Gonzalez-Fernandez and B. Ermentrout, Math. Biosci. **119**, 127 (1994).

[28] D. Parthimos, D. H. Edwards, and T. M. Griffith, Am. J. Physiol.: Heart Circ. Physiol. **277**, H1119 (1999).

[29] M. Koenigsberger, R. Sauser, M. Lamboley, J. L. Beny, and J. Meister, Biophys. J. **87**, 92 (2004).

[30] J. P. Johny and T. David, in Proceedings of World Congress on Research and Innovations, Thrissur, India, 2013, available at http://ir.canterbury.ac.nz/handle/10092/10508.

[31] A. Kapela, J. Parikh, and N. M. Tsoukias, Biophys. J. **102**, 211 (2012).

[32] L. Xiang and R. L. Hester, *Cardiovascular Responses to Exercise* (Morgan & Claypool Life Sciences, 2012).

[33] Y. Y. L. Wang, M. Y. Jan, C. S. Shyu, C. A. Chiang, and W. K. Wang, IEEE Trans. Biomed. Eng. **51**, 193 (2004).

[34] See https://drive.google.com/open?id=0B8l8iii7Z4iqWWJRLTduRl9zMVE.

[35] See http://www.physiome.org/jsim.

[36] A. Schuster, M. Lamboley, C. Grange, H. Oishi, J. L. Beny, N. Stergiopulos, and J. J. Meister, J. Cardiovasc. Pharmacol. **43**, 539 (2004).

[37] W. F. Jackson, Blood Vessels **25**, 144 (1988).

[38] K. Fujii, D. D. Heistad, and F. M. Faraci, Am. J. Physiol. **258**, H1829 (1990).

[39] H. Gustafsson, A. Bulow, and H. Nilsson, Acta Physiol. Scand. **152**, 145 (1994).

[40] K. A. Dora, J. M. Hinton, S. D. Walker, and C. J. Garland, Br. J. Pharmacol. **129**, 381 (2000).

[41] K. Okazaki, S. Seki, N. Kanaya, J. Hattori, N. Tohse, and A. Namiki, Anesthesiology **98**, 1164 (2003).

[42] J. R. Mauban and W. G. Wier, Am. J. Physiol.: Heart Circ. Physiol. **287**, H608 (2004).

[43] H. Peng, V. Matchkov, A. Ivarsen, C. Aalkjaer, and H. Nilsson, Circ. Res. **88**, 810 (2001).

[44] I. S. Bartlett, G. J. Crane, T. O. Neild, and S. S. Segal, J. Vasc. Res. **37**, 568 (2000).

[45] H. Oishi, A. Schuster, W. Lamboley, N. Stergiopulos, J. J. Meister, and J. L. Beny, Life Sci. **71**, 2239 (2002).

[46] L. K. Moore and J. M. Burt, Am. J. Physiol. **269**, H1481 (1995).

[47] M. J. Mulvany, U. Baandrup, and H. J. Gundersen, Circ. Res. **57**, 794 (1985).

[48] C. D. Benham and T. B. Bolton, J. Physiol. **381**, 385 (1986).

[49] M. Koenigsberger, D. Seppey, J. L. Beny, and J. J. Meister, Biophys. J. **99**, 333 (2010).